# Metabolic profiling of visceral adipose tissue from obese subjects with or without metabolic syndrome

**Article** *in* Biochemical Journal · February 2018

DOI: 10.1042/BCJ20170604

CITATIONS
11

READS
220

**12 authors**, including:

Manfredi Tesauro
University of Rome Tor Vergata
**157** PUBLICATIONS **3,913** CITATIONS
SEE PROFILE

Carmine Cardillo
Catholic University of the Sacred Heart
**152** PUBLICATIONS **5,296** CITATIONS
SEE PROFILE

Giuseppe Sica
University of Rome Tor Vergata
**213** PUBLICATIONS **2,474** CITATIONS
SEE PROFILE

Paolo Gentileschi
University of Rome Tor Vergata
**136** PUBLICATIONS **3,031** CITATIONS
SEE PROFILE

*Biochemical Journal* (2018) **475** 1019–1035
https://doi.org/10.1042/BCJ20170604

Research Article

# Metabolic profiling of visceral adipose tissue from obese subjects with or without metabolic syndrome

Eleonora Candi[1,2,*], Manfredi Tesauro[3,*], Carmine Cardillo[4], Anna Maria Lena[1], Francesca Schinzari[4], Giuseppe Rodia[3], Giuseppe Sica[1], Paolo Gentileschi[1], Valentina Rovella[3], Margherita Annicchiarico-Petruzzelli[2], Nicola Di Daniele[3] and Gerry Melino[1,5]

[1]Department of Experimental Medicine and Surgery, University of Rome 'Tor Vergata', 00133 Rome, Italy; [2]Biochemistry Laboratory, Istituto Dermopatico Immacolata (IDI-IRCCS), 00100 Rome, Italy; [3]Department of Systems Medicine, University of Rome 'Tor Vergata', 00133 Rome, Italy; [4]Department of Internal Medicine, Catholic University, 00168 Rome, Italy; [5]Medical Research Council, Toxicology Unit, Hodgkin Building, Leicester University, Lancaster Road, PO Box 138, Leicester LE1 9HN, U.K.

**Correspondence:** Nicola Di Daniele (didaniele@med.uniroma2.it) or Gerry Melino (melino@uniroma2)

Obesity represents one of the most complex public health challenges and has recently reached epidemic proportions. Obesity is also considered to be primarily responsible for the rising prevalence of metabolic syndrome, defined as the coexistence in the same individual of several risk factors for atherosclerosis, including dyslipidemia, hypertension and hyperglycemia, as well as for cancer. Additionally, the presence of three of the five risk factors (abdominal obesity, low high-density lipoprotein cholesterol, high triglycerides, high fasting glucose and high blood pressure) characterizes metabolic syndrome, which has serious clinical consequences. The current study was conducted in order to identify metabolic differences in visceral adipose tissue (VAT) collected from obese (body mass index 43–48) human subjects who were diagnosed with metabolic syndrome, obese individuals who were metabolically healthy and nonobese healthy controls. Extensive gas chromatography/mass spectrometry (GC/MS) and liquid chromatography/mass spectrometry (LC/MS/MS) analyses were used to obtain the untargeted VAT metabolomic profiles of 481 metabolites belonging to all biochemical pathways. Our results indicated consistent increases in oxidative stress markers from the pathologically obese samples in addition to subtle markers of elevated glucose levels that may be consistent with metabolic syndrome. In the tissue derived from the pathologically obese subjects, there were significantly elevated levels of plasmalogens, which may be increased in response to oxidative changes in addition to changes in glycerolphosphorylcholine, glycerolphosphorylethanolamine glycerolphosphorylserine, ceramides and sphingolipids. These data could be potentially helpful for recognizing new pathways that underlie the metabolic–vascular complications of obesity and may lead to the development of innovative targeted therapies.

## Introduction

Patients with obesity-related pathophysiologies such as insulin resistance and the metabolic syndrome show a markedly increased risk for type 2 diabetes and atherosclerotic cardiovascular disease. This risk appears to be linked to different alterations in adipose tissue function leading to a chronic inflammation and to the dysregulation of adipocyte-derived factors. Insulin resistance and the resultant hyperinsulinemia lead to a series of alterations in different pathways that are the basis of many obesity-related complications. Interestingly, the obese phenotype has a high degree of heterogeneity, spanning a wide range from metabolically healthy obesity to the combination of several metabolic and circulatory abnormalities known as the metabolic syndrome. Given the different cardiovascular outcomes associated with metabolically healthy and 'at risk' obesity, there is an urgent need to better understand how obesity causes diabetes and atherosclerotic complications. The specific molecular

*Co-first authors.

Received: 12 August 2017
Revised: 30 January 2018
Accepted: 31 January 2018

Accepted Manuscript online: 8 February 2018
Version of Record published: 15 March 2018

Biochemical Journal (2018) 475 1019–1035
https://doi.org/10.1042/BCJ20170604

mechanisms that lead from obesity toward a greater risk of cardiometabolic complications or even cancer remain elusive. The characterization of the mechanisms involved in the pathophysiology of obesity and insulin resistance have become a pressing challenge and could lead to the successful development of targeted therapies.

Oxidative stress, inflammation and the dysregulation of multiple lipid metabolic pathways are closely interlinked in obesity and seem to be key factors in the pathogenesis of obesity-associated illnesses [1–7]. In particular, excessive food intake leads to mitochondrial dysfunction, in part due to the effects of high concentrations of reactive oxygen species and the consequent oxidative stress, which plays a central role in the development of insulin resistance [8–10] in different clinical conditions, such as obesity, type 2 diabetes and metabolic syndrome [11–14]. In turn, mitochondrial dysfunction increases the levels of intracellular FA metabolites (fatty acyl-CoA, diacylglyerol) that alter insulin signaling in the muscle as well as in the liver [15–18]. Recently, great interest has emerged regarding the dysregulation of adipose tissue function in obesity-related complications, particularly with regard to bioactive lipids synthesized in adipose tissue, including sphingolipids and phospholipids, as well as in fatty acids derived from the phospholipids of the cell membrane [19]. While abdominal obesity is determined by the accumulation of both subcutaneous adipose tissue and visceral adipose tissue (VAT), several evidence demonstrates that VAT rather than subcutaneous adipose tissue plays a more significant pathogenic role in metabolic disease producing many adipokines and cytokines leading to a proinflammatory, procoagulant and insulin-resistant state [20–22]. To investigate the metabolic changes directly in VAT, we used a wide metabolomic approach to identify individual metabolites and thus discrete pathways in normal versus obese subjects. The application of metabolomics in obesity was also used to evaluate the therapeutic effect of various pharmacological and lifestyle-related strategies involved in obesity-related vascular complications. The goal of the present study was to interrogate the biochemical profiles of human VAT originating from healthy subjects and an obese cohort stratified by the clinical diagnosis of metabolic syndrome, with the aim of characterizing the altered metabolism associated with the pathology of metabolic syndrome.

# Materials and methods

## Study population

The present study included 53 patients admitted to the surgical unit of the University of Rome Tor Vergata for bariatric or general surgery. The project was approved by the Medical Ethics Committee of the Institution. Written and informed consent was obtained from all participants before they were included in the study. The patients were divided into three study groups as indicated in Table 1 and Supplementary Table S1. *Group 1*: 17 healthy (H) subjects, body mass index (BMI) = 25.31 ± 0.91, normal waist circumference, matched to the obese groups for approximate age and sex. *Group 2*: 18 obese patients without metabolic syndrome, indicated as obese (O). *Group 3*: 18 patients with obesity-related metabolic syndrome (indicated as pathologically obese, PO) defined according to the National Cholesterol Education Program's Adult Treatment Panel III report (ATP III) [23]. Metabolic syndrome is present if three or more of the following five criteria are met: waist circumference over 40 inches (men) or 35 inches (women), blood pressure over 130/85 mmHg, fasting triglyceride level over 150 mg/dl, fasting high-density lipoprotein (HDL) cholesterol level less than 40 mg/dl (men) or 50 mg/dl (women) and fasting blood sugar over 100 mg/dl. Increased waist circumference was present in all PO patients, lipid abnormalities were present in 17 patients, hypertension was present in 7 patients and impaired glucose tolerance was present in 12 patients. Each subject was screened according to clinical history, physical examination, ECG, chest X-ray and routine chemical analyses. None of the participants in the healthy subjects group had evidence of present or past hypertension, hyperlipidemia, diabetes, cardiovascular disease or any other systemic condition. No particular diet has been recommended to the patients before bariatric or general surgery. Overall exclusion criteria were acute or chronic infection, acute or chronic autoimmune inflammatory disease, history of cancer and history of alcohol or drug dependence; for a summary of the clinical features and patient's habits, see Tables 2 and 3 and Supplementary Table S1. Plasma parameters were evaluated in fasting conditions.

## Sample preparation

Samples were inventoried and immediately stored at −80°C. Each sample was accessioned into the Metabolon LIMS system and was assigned by the LIMS a unique identifier that was associated with the original source identifier only. This identifier was used to track all sample handling, tasks and results. The samples (and all derived aliquots) were tracked by the LIMS system. All portions of any sample were automatically assigned

Biochemical Journal (2018) **475** 1019–1035
https://doi.org/10.1042/BCJ20170604

**Table 1 Experimental design**

| Group | No. of patients | Description |
|---|---|---|
| H (healthy) | 17 (6M/11F) | Healthy subjects |
| O (obese) | 18 (4M/14F) | Obese subjects without metabolic syndrome |
| PO (pathological obese) | 18 (8M/10F) | Obese subjects with metabolic syndrome |

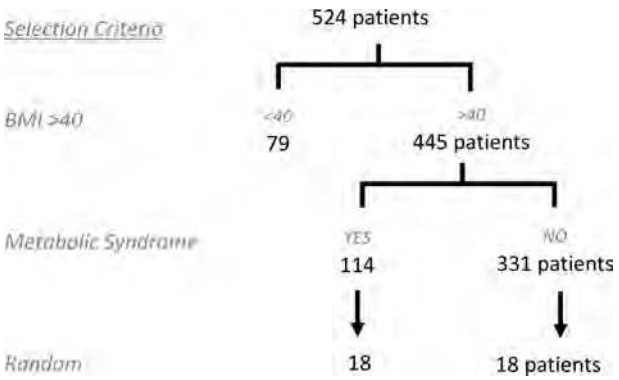


M/F: male and female. Age, years: >20; <65.

their own unique identifiers by the LIMS when a new task was created; the relationship between these samples was also tracked. All samples were maintained at −80°C until they were processed. Samples were prepared using the automated MicroLab STAR® system from Hamilton Company. Several recovery standards were added prior to the first step in the extraction process for QC purposes. To remove protein, dissociate small molecules bound to protein or to remove those trapped in the precipitated protein matrix and to recover chemically diverse metabolites, proteins were precipitated with methanol under vigorous shaking for 2 min (Glen Mills GenoGrinder 2000) followed by centrifugation.

## Metabolomic analysis

The extracted samples were divided into five fractions: two for analysis by two separate reverse-phase (RP)/UPLC–MS/MS methods with positive ion mode electrospray ionization (ESI), one for analysis by RP/UPLC–MS/MS with negative ion mode ESI, one for analysis by HILIC/UPLC–MS/MS with negative ion mode ESI and one sample was reserved for backup. Samples were placed briefly on a TurboVap® (Zymark) to remove the organic solvent. The sample extracts were stored overnight under nitrogen before preparation for analysis. For further details on data quality and process variability, see the 'Supplementary Materials and Methods' section.

**Table 2 Clinical characteristic of study population**
Plasma measurements were performed in fasting conditions. For each group, mean (±SD) is reported. *t*-Test (*$P < 0.05$) evaluated between groups O and PO.

| | Healthy (H) | Obese (O) | Pathological obese (PO) |
|---|---|---|---|
| MAP (mmHg) | 96.56 ± 1.60 | 95.46 ± 1.76 | 95.46 ± 1.76 |
| Waist (cm) | 86.23 ± 1.24 | 106.66 ± 1.70 | 105.11 ± 1.35 |
| BMI (kg/m$^2$) | 25.31 ± 0.91 | 43.16 ± 1.57 | 48.59 ± 1.72* |
| Glycemia (mg/dl) | 85.17 ± 1.89 | 88.11 ± 2.48 | 136.11 ± 12.12* |
| HDL (mg/dl) | 46.47 ± 3.66 | 49.66 ± 2.88 | 37.72 ± 2.82* |
| Triglycerides (mg/dl) | 107.29 ± 7.30 | 110.33 ± 10.14 | 230.83 ± 28.45* |

Abbreviations: MAP: mean arterial pressure; BMI: body mass index; HDL: high-density lipoprotein.

Biochemical Journal (2018) 475 1019–1035
https://doi.org/10.1042/BCJ20170604

**Table 3 Selected clinical features/conditions of population study**

| | Healthy (H) | Obese (O) | Pathological obese (PO) |
|---|---|---|---|
| Hypertension | 0/17 | 0/18 | 16/18 |
| Hyperlipidemia | 0/17 | 4/18 | 5/18 |
| Diabetes | 0/17 | 0/18 | 12/18 |
| Hypothyroidism | 1/17 | 4/18 | 1/18 |
| Gallstones | 5/17 | 0/18 | 0/18 |
| Asthma | 0/17 | 2/18 | 1/18 |
| Smoking | 6/17 | 9/18 | 9/18 |
| Contraception | 1/17 | 2/18 | 0/18 |
| Favism | 1/17 | 0/18 | 0/18 |
| Diverticulosis | 0/17 | 1/18 | 0/18 |
| Osteoporosis | 1/17 | 0/18 | 3/18 |
| Osas | 0/17 | 0/18 | 1/18 |

### Pathway enrichment analysis

For each individual pair-wise comparison, pathway enrichment displays the number of experimentally regulated compounds relative to all detected compounds in a pathway, compared with the total number of experimentally regulated compounds relative to all detected compounds in the study. A pathway enrichment value (PEV) greater than one indicates that the pathway contains more experimentally regulated compounds relative to the study overall, suggesting that the pathway may be a target of interest related to the experimental perturbation. Enrichment: (# of significant metabolites in pathway ($k$)/total # of detected metabolites in pathway ($m$))/(total # of significant metabolites ($n$)/total # of detected metabolites ($N$)) ($k/m$)/($n/N$).

## Results

### Clinical parameters and global metabolic profiling

The present study consisted of 53 patients divided into three groups: healthy (H), healthy obese (O) and pathologically obese (PO) (Table 1). The clinical parameters used to select subjects are shown in Tables 1–3 and Supplementary Table S1. As a control, we collected abdominal adipose tissue from 17 healthy subjects (H), BMI = 25.31 ± 0.91, with a normal waist circumference, matched to the obese groups for approximate age and sex. Then, we collected 18 healthy obese patients without metabolic syndrome, indicated as obese (O), and 18 patients with obesity-related metabolic syndrome, indicated as pathologically obese (PO). The latter group was defined according to the National Cholesterol Education Program's Adult Treatment Panel III report (ATP III) [23]. Increased waist circumference was present in all PO and O patients, lipid abnormalities were present in 16/18 PO patients, hypertension was present in 16/18 PO patients and diabetes was present in 12/18 PO patients (Table 3). Based on gas chromatography/mass spectrometry (GC/MS) and liquid chromatography/mass spectrometry (LC/MS/MS) analyses, 481 compounds of known identity were identified in adipose tissue (Table 4 and Supplementary Table S2). A summary of the metabolites that achieved statistical significance ($P \leq 0.05$), as well as those approaching significance ($0.05 < P < 0.10$), is shown in Supplementary Table S2. Some of these metabolites are involved in the pathways described below. General platform methods, data analysis and metabolite detection identification are described in the 'Materials and Methods' and 'Supplementary Material' sections.

Random forest (RF) analysis shows limited but significant separation between groups. To analyze segregation between groups, we performed RF analysis. RF analysis showed a moderate ability to segregate obese from healthy controls. Segregation between O and PO patients was less prevalent (Supplementary Figure S1). RF analysis is an unbiased and supervised classification technique based on an ensemble of a large number of decision trees. Using the primary groupings of O, PO and healthy controls, RF classification analysis of the metabolic profiles of the VAT resulted in a 71% and 80% predictive accuracy in differentiating the O and PO samples, respectively, from the healthy controls (Supplementary Figure S1). The outcomes of these RF analyses

**Table 4 Summary of metabolites change**
Color code indicates statistically significant increase (red) or decrease (green). A total of 197 metabolites changed in a statistically significant manner.

| Significantly altered metabolites | Group effect | Obese/ healthy (O/H) | Pathological obese/ healthy (PO/H) | Pathological obese/ obese (PO/O) |
|---|---|---|---|---|
| Total metabolites $P \leq 0.05$ | 197 | 206 | 112 | 87 |
| Metabolites | — | 2/204 | 19/93 | 86/1 |
| Total metabolites $0.05 < P < 0.10$ | 49 | 45 | 49 | 48 |
| Metabolites | — | 2/43 | 9/40 | 46/2 |

were better than random chance alone (50% accuracy for two groups), indicating differences in the metabolite profiles of the obese groups compared with healthy controls. In contrast, the RF classification between the O and PO resulted in a lower predictive accuracy of 69%, and while this is greater than one would expect due to random chance alone, it does suggest that these groups have limited segregation (Supplementary Figure S1). RF analysis also produced a list of metabolites ranked by their importance to the classification scheme. The primary class of molecule found to segregate between the O and PO samples was lipids, which included many lysoplasmalogens (discussed later). Although there was limited segregation between groups, changes in metabolites were analyzed as PEVs obtained via the differential enrichment pathways among groups (Figure 1). A comparison of PO versus H subjects and PO versus O subjects revealed significantly different metabolites according to the pathway enrichment value (PEV). In the first group (Figure 1a), we found high PEV in the following pathways: acetylated peptides, creatinine metabolism, eicosanoid, glycogen metabolism, hemoglobin and porphyrin metabolism, inositol metabolism and ketone bodies. In the second group (Figure 1b), we found high PEV in ceramide, phosphatidylserine, glutathione, amino sugar metabolism, plasmalogen, sphingolipid and phospholipid metabolism and γ-glutamyl amino acid metabolism. These findings confirm the presence of significantly altered metabolic pathways in different patient groups.

## Indications of increased oxidative stress in pathologically obese individuals in relation to obese individuals

Here, we detected differential levels of metabolites which confirmed different levels of oxidative stress in adipose tissue from PO and O subjects (Figure 2a–m). PO tissue samples exhibited lower levels of glutathione (GSH), although this did not achieve significance, and elevated levels of oxidized glutathione (GSSG, $P \leq 0.05$) when compared with O samples. This may highlight a difference in redox homeostasis between both groups of obese subjects. Furthermore, modestly higher levels of cysteine-glutathione disulfide (marker of free radical exposure, $0.05 < P < 0.10$) as well as methionine sulfone ($P \leq 0.05$), *N*-acetylmethionine sulfoxide ($0.05 < P < 0.10$) and cysteine (the oxidized form of cysteine, $P \leq 0.05$) in the PO samples in relation to O further support increased oxidative stress. High levels of ophthalmate ($P \leq 0.05$), a tripeptide analog of GSH in which cysteine has been replaced by 2-aminobutyrate that is also considered a marker of oxidative stress, were also detected in PO samples. Aside from direct free radical detoxification, GSH can be utilized for the generation of γ-glutamyl amino acids. γ-Glutamyl amino acids regulate the exchange of intra- and extracellular GSH and are generated via γ-glutamyl transferase (GGT) through the transfer of a γ-glutamyl moiety of glutathione to an amino acid acceptor. The extracellular metabolism of GSH by GGT promotes the release and recovery of constituent amino acids, such as glutamate and cysteine. Thus, GGT functions as a source of essential amino acids both for protein synthesis and for the maintenance of intracellular levels of GSH. As noted in the heatmap (Supplementary Table S2), there were significantly higher levels of many γ-glutamyl amino acids, including γ-glutamylglutamine ($P \leq 0.05$), γ-glutamylthreonine ($P \leq 0.05$) and γ-glutamylvaline ($P \leq 0.05$), along with higher levels of the GSH catabolite 5-oxoproline ($P \leq 0.05$) (Figure 2h–k), which may be indicative of γ-glutamyl amino acid degradation in an attempt to restore cysteine and GSH levels. Interestingly, many of these changes were not found to be significantly different between the PO and O subjects. Surprisingly, the majority of the metabolites included in Figure 2 were similar between the PO and H groups in comparison

Biochemical Journal (2018) **475** 1019–1035
https://doi.org/10.1042/BCJ20170604

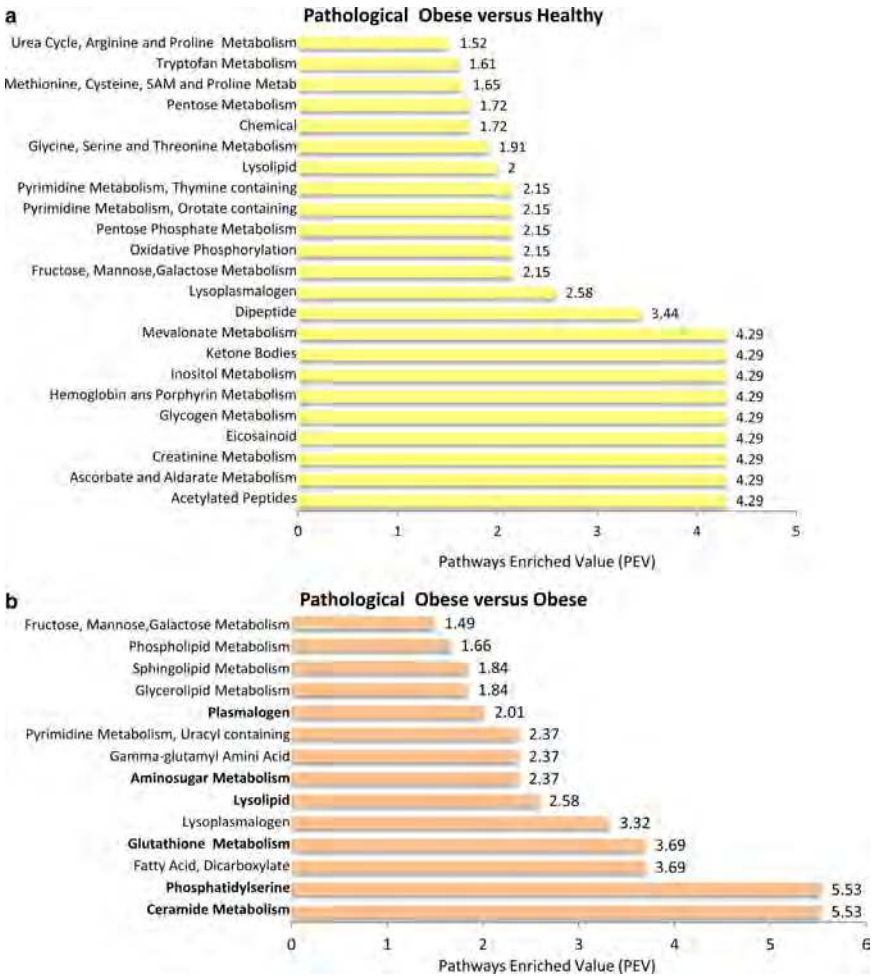


**Figure 1. Biochemical changes in adipose tissue from groups evaluated as the pathway enrichment value (PEV).**
Metabolite changes were expressed as the pathway enrichment value (PEV). Values are based on the significantly regulated metabolites ($P < 0.05$) from the different groups. (**a**) Pathologically obese *versus* healthy and (**b**) pathologically obese *versus* obese relative to all detected compounds in the pathway. PEV = $k/m/n/N$, $k$ = number of significant metabolites in pathway, $m$ = total number of detected metabolites in pathway, $n$ = total number of significant metabolites, $N$ = total number of detected metabolites. Detailed statistics are shown in Supplementary Table S2.

with O and H groups (see Supplementary Table S2). For example, the levels of γ-glutamylvaline and cysteine-glutathione disulfide did not significantly changed between PO *versus* H (fold change 1.131 and 0.778, respectively), while significantly changed between O *versus* H (fold change 0.662, and 0.553, respectively; $P \leq 0.05$; Supplementary Table S2). This could be due to biological variability between samples or may indicate a compensatory and/or adaptation mechanism toward oxidative stress in PO subjects VAT. Another important finding of our study was the significant differences in lipid metabolites, including ceramides, sphingosine, sphingomyelins and plasmalogens in the pathologically obese subjects.

## Ceramide and sphingolipid metabolism

Obesity is associated with the accumulation of lipid metabolites in organs, including the liver and the heart. These lipids, including ceramides, are critical for obesity-induced pathologies [24]. All of the detected ceramides [ceramide (d14: 1/22 : 0, d16: 1/20 : 0; $P \leq 0.05$), ceramide (d18: 1/14 : 0, d16: 1/16 : 0; $P \leq 0.05$), ceramide (d18: 1/17 : 0, d17: 1/18 : 0; $P \leq 0.05$) and ceramide (d18: 1/20 : 0, d16: 1/22 : 0, d20: 1/18 : 0; $P \leq 0.05$)] were found to be significantly higher in PO samples compared with O samples (Figure 3a–d). These metabolite changes were not significantly altered comparing O *versus* H and PO *versus* H groups (fold change ranging

Biochemical Journal (2018) **475** 1019–1035
https://doi.org/10.1042/BCJ20170604

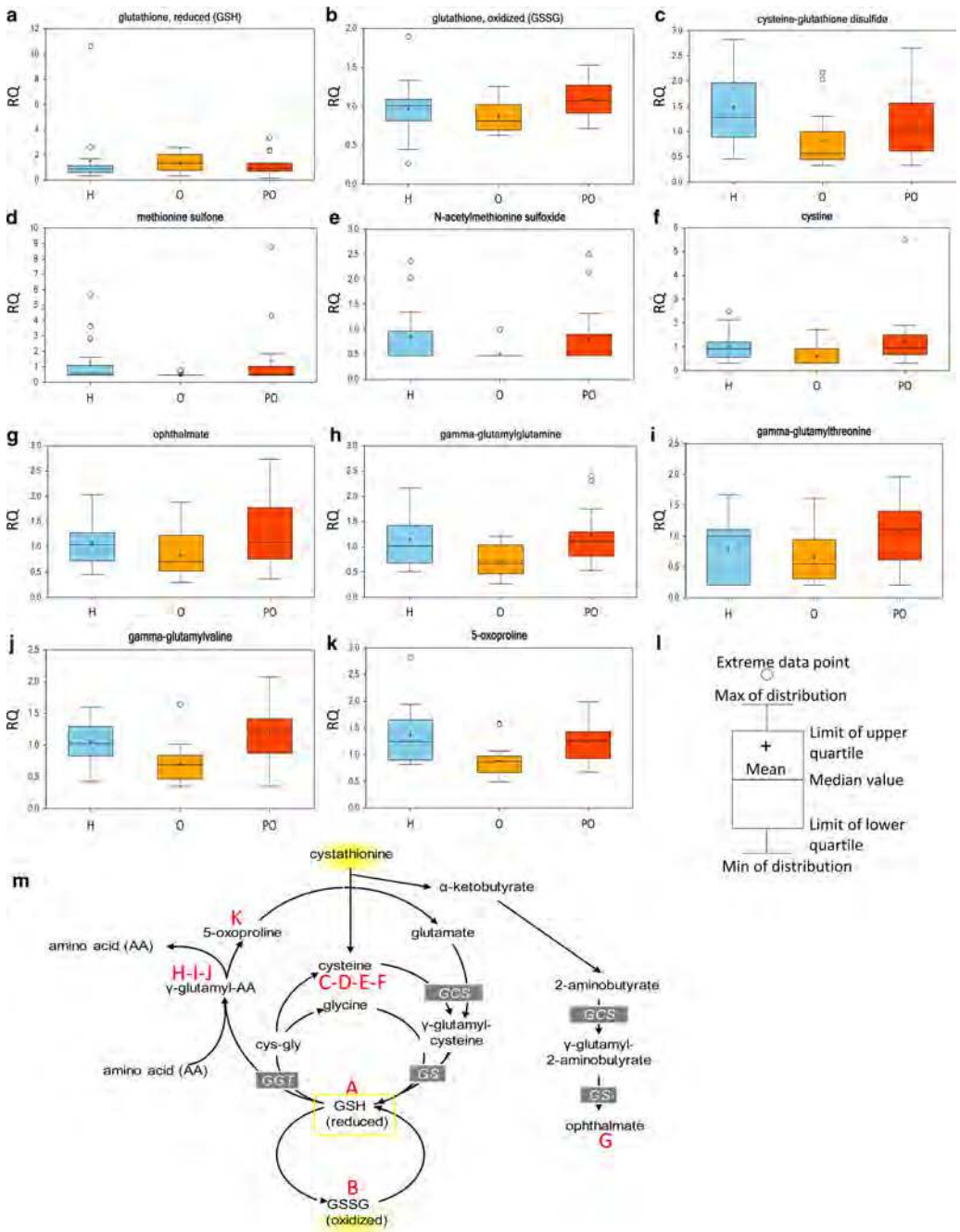


**Figure 2. Oxidative stress is increased in pathologically obese samples.**

The levels of reduced glutathione (GSH) (**a**), oxidized glutathione (GSSG) (**b**), cysteine-glutathione disulfide (**c**), methionine sulfone (**d**), *N*-acetylmethionine sulfoxide (**e**), cysteine (**f**), ophthalmate (**g**), γ-glutamylgluatmine (**h**), γ-glutamylthreonine (**i**), γ-glutamylvaline (**j**) and 5-oxoproline (**k**) were measured as described in the Materials and Methods. The box legend is shown in (**l**). Pathway connections of the cited metabolites are shown in (**m**). H, healthy; O, obese; PO, pathologically obese. GGT, γ-glutamyl transferase; GS, glutathione synthetase; GCS, glutamylcysteine synthetase. Data have been plotted in the whisker plots. Detailed statistics are shown in Supplementary Table S2.

from 0.869 to 1.269; Supplementary Table S2), indicating that they are specific for PO subjects. Other sphingosines and sphingomyelins (behenoyl sphingomyelin, tricosanoyl sphingomyelin and lignoceroyl sphingomyelin) were also found to be significantly ($P \leq 0.05$) higher within the PO group compared with the O group

Biochemical Journal (2018) **475** 1019–1035
https://doi.org/10.1042/BCJ20170604

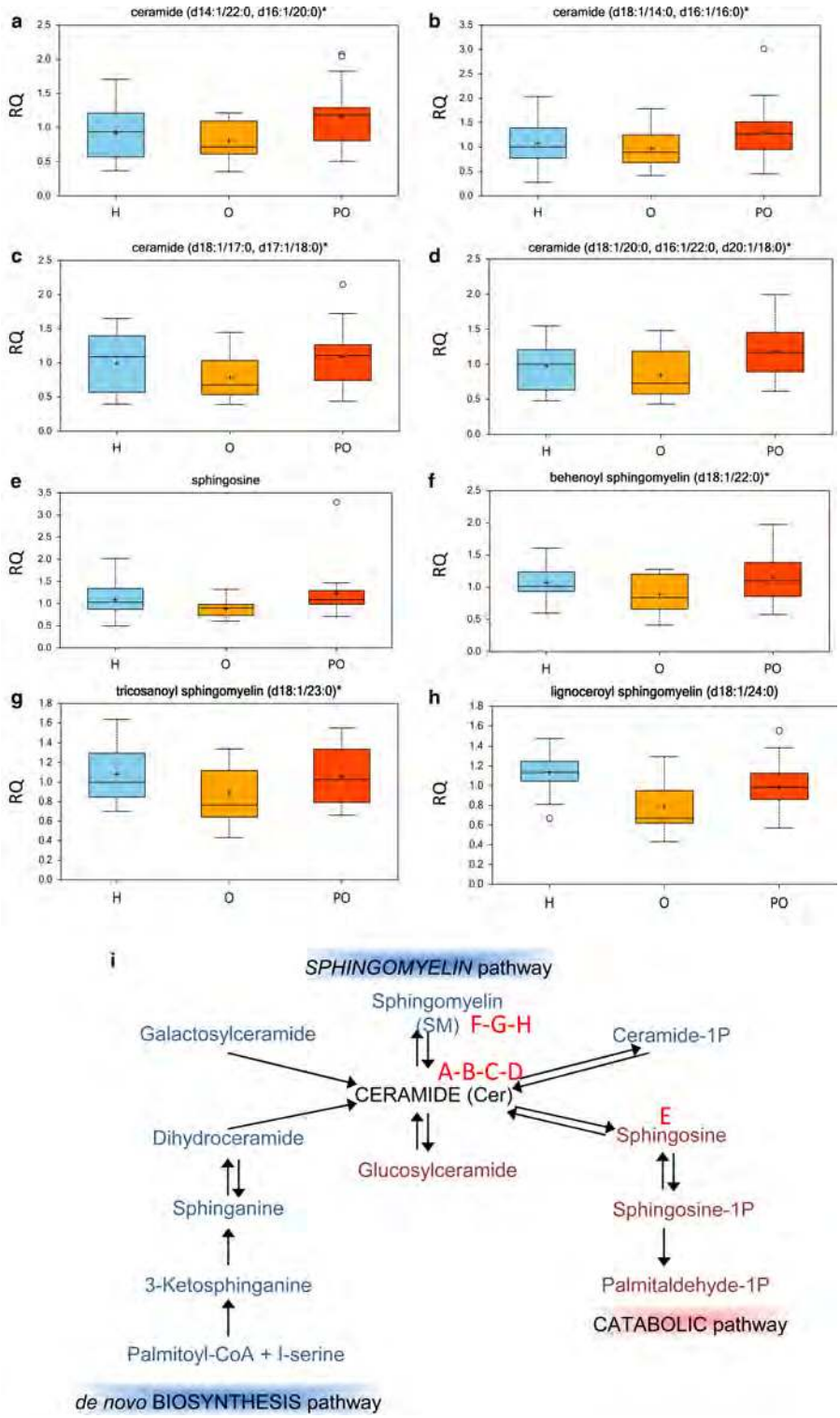


**Figure 3. Ceramide and sphingolipid metabolism are increased in pathologically obese adipose tissue.**
Increased levels of ceramide (**a–d**), sphingosine (**e**) and sphingomyelin derivatives (**f–h**) were detected in pathologically obese adipose tissue versus obese tissue. Pathway connections of the cited metabolites are shown in (**i**). The box legend is as indicated in Figure 2I. H, healthy; O, obese; PO, pathologically obese. Data have been plotted in the whisker plots. Detailed statistics are shown in Supplementary Table S2.

(Figure 3e–i). While sphingosine was not significantly altered comparing O *versus* H and PO *versus* H groups (fold change 0.815 and 1.227, respectively), behenoyl sphingomyelin, tricosanoyl sphingomyelin and lignoceroyl sphingomyelin metabolite changes decreased significantly O *versus* H groups (fold change 0.832, 0.815 and 0.695, respectively; $P \leq 0.05$). Sphingolipids are part of the cell membrane and are components of lipid rafts. They also serve as bio-effector molecules involved in cell proliferation. These changes may be consistent with putative changes in sphingolipid intake and turnover. Interestingly, ceramides are lipid metabolites that accumulate in tissues in response to obesity, and pharmacological strategies that reduce ceramide levels in tissues improve metabolic health [21]. These molecules may also be associated with inflammation, which would be consistent with the slightly higher levels of the eicosanoid 15-HETE and prostaglandins (Figure 4a,b). 15-HETE and 6-ketoprostaglandin F1alpha were significantly up-regulated in PO *versus* H subjects (fold change 1.263 and 1.740, respectively; $P \leq 0.05$), while slightly higher levels were detected in O subjects (Supplementary Table S2) without reaching statistical significance.

## Plasmalogens and lysoplasmalogens

Plasmalogens are a class of membrane glycerophospholipids containing a fatty alcohol with an ether bond at the sn-1 position that are enriched in polyunsaturated fatty acids at the sn-2 position [25]. Many detected plasmalogens, including 1-(1-enyl-palmitoyl)-2-palmitoyl-GPC (glycerolphosphorylcholine), 1-(1-enyl-palmitoyl)-2-arachidonyl-GPC, 1-(1-enyl-palmitoyl)-2-arachidonyl-GPE (glycerolphosphorylethanolamine) and 1-(1-enyl-stearoyl)-2-arachidonoyl-GPE, were found to be significantly ($P \leq 0.05$) greater in PO samples compared with those from H and O subjects (Table 5), indicating that the increase of these metabolite might be specific for PO subjects. Plasmalogens are known to be involved in protecting mammalian cells from redox damage and may be elevated in response to the previously described indicators of oxidative stress. Plasmalogens are also anti-inflammatory and serve as lipid signaling molecules. Their production may be a compensatory response to the development of metabolic syndrome. Plasmalogen levels increase as a consequence of inflammation and metabolic changes. This seems to be related to immuno-metabolism, linking immunological/inflammation conditions to metabolic diseases. Therefore, plasmalogens can be used as biomarkers for early disease detection and later to monitor disease progress [26]. Additionally, lysoplasmalogens, in which the sn-2 acyl chain has been cleaved, were also found to be significantly elevated in PO samples compared with O and H samples. Among them, 1-(1-enyl-palmitoyl)-GPE, 1-(1-enyl-oleoyl)-GPE and 1--(1-enyl-stearoyl)-GPE were elevated ($P < 0.05$, Table 5) in PO (fold change ranging from 1.275 to 1.893, $P < 0.05$). This is likely due to increased lipase activity in PO versus H and O groups, possibly as a mechanism to increase fatty acid levels.

## Phospholipids and lysolipids

The most abundant lipid components of the cell membrane are phospholipids. We detected many phospholipids that were significantly ($P \leq 0.05$) higher in the PO tissue compared with tissue from obese (O) subjects (Table 6). Among these, we found glycerolphosphorylcholine (GPC), glycerolphosphoethanolamine, 1,2-dipalmitoyl-GPC, 1-stearoyl-2-arachidonoyl-GPC, 1-palmitoyl-2-arachidonoyl-GPC, 1-steroyl-2-arachidonoyl-GPI (glycerolphosphorylinositol), 1-steroyl-2-arachidonoyl-GPE, 1-palmitoyl-2-steroyl-GPC, 1-stearoyl-2-oleoyl-GPG

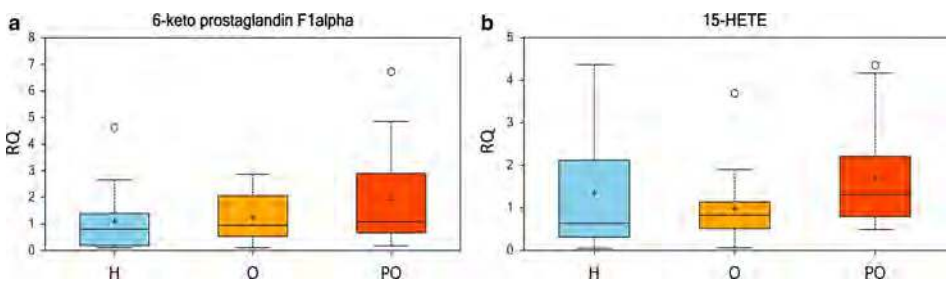


**Figure 4. Inflammatory markers increase in obese and in pathologically obese samples.**

The levels of prostaglandins (**a**) and 15-HETE (**b**) were observed in pathologically obese adipose tissue and obese tissue compared with samples from healthy subjects. The box legend is as indicated in Figure 2l. H, healthy; O, obese; PO, pathologically obese. Data have been plotted in the whisker plots. Detailed statistics are shown in Supplementary Table S2.

Biochemical Journal (2018) 475 1019–1035
https://doi.org/10.1042/BCJ20170604

**Table 5 Plasmalogen and lysoplasmalogen**

| Sub pathway | Biochemical name | Fold of change | | |
|---|---|---|---|---|
| | | O/H | PO/H | PO/O |
| Plasmalogen | 1-(1-Eenyl-palmitoyl)-2-oleoyl-GPE (P-16:0/18:1) | 0.9598 | 1.0265 | 1.0695 |
| | 1-(1-Enyl-palmitoyl)-2-linoleoyl-GPE (P-16:0/18:2) | 0.9408 | 0.8587 | 0.9127 |
| | 1-(1-Enyl-palmitoyl)-2-palmitoyl-GPC (P-16:0/16:0) | 0.7662 | 1.3105 | 1.7103 |
| | 1-(1-Enyl-palmitoyl)-2-palmitoleoyl-GPC (P-16:0/16:1) | 0.9391 | 1.269 | 1.3513 |
| | 1-(1-Enyl-palmitoyl)-2-arachidonoyl-GPE (P-16:0/20:4) | 0.9845 | 1.3144 | 1.3352 |
| | 1-(1-Enyl-palmitoyl)-2-oleoyl-GPC (P-16:0/18:1) | 0.794 | 1.0023 | 1.2624 |
| | 1-(1-Enyl-stearoyl)-2-oleoyl-GPE (P-18:0/18:1) | 0.7632 | 0.7778 | 1.019 |
| | 1-(1-Enyl-stearoyl)-2-linoleoyl-GPE (P-18:0/18:2) | 0.7595 | 0.6394 | 0.8419 |
| | 1-(1-Enyl-palmitoyl)-2-arachidonoyl-GPC (P-16:0/20:4) | 0.8315 | 1.3102 | 1.5756 |
| | 1-(1-Enyl-palmitoyl)-2-linoleoyl-GPC (P-16:0/18:2) | 0.8564 | 1.1088 | 1.2947 |
| | 1-(1-Enyl-stearoyl)-2-arachidonoyl-GPE (P-18:0/20:4) | 0.8307 | 1.12 | 1.3483 |
| Lysoplasmalogen | 1-(1-Enyl-palmitoyl)-GPE (P-16:0) | 0.8126 | 1.6608 | 2.0438 |
| | 1-(1-Enyl-oleoyl)-GPE (P-18:1) | 0.7024 | 1.6888 | 2.4044 |
| | 1-(1-Enyl-stearoyl)-GPE (P-18:0) | 0.6738 | 1.2756 | 1.8931 |
| | 1-(1-Enyl-oleoyl)-2-oleoyl-GPE (P-18:1/18:1) | 0.8247 | 0.9042 | 1.0964 |
| | 1-(1-Enyl-oleoyl)-2-linoleoyl-GPE (P-18:1/18:2) | 0.8442 | 0.7229 | 0.8563 |
| Glycerolipid metabolism | Glycerol | 0.7238 | 0.825 | 1.1398 |
| | Glycerol 3-phosphate | 0.8259 | 0.9142 | 1.1069 |
| | Glycerophosphoglycerol | 0.8827 | 1.1881 | 1.346 |

Values in the table indicate ratio.
Green indicates significant differences ($P \leq 0.05$) between groups shown, metabolite ratio <1.00.
Red indicates significant differences ($P \leq 0.05$) between groups shown, metabolite ratio ≥1.00.
Non-colored: mean values are not significantly different for that comparison.

and 1-stearoyl-2-linoleoyl-GPS (glycerolphosphorylserine) to be increased. Interestingly, phospholipid metabolism did not significantly changed comparing PO versus H groups (Table 6), except for an increase of GPC (fold change 1.376, $P \leq 0.05$) and a decrease of glycerophosphoinositol, 1,2-dilinoleoyl-GPC, 1-oleoyl-2-linoleoyl-GPE and 1--linoleoyl-2-arachidonoyl-GPC (fold change 0.608, 0.617, 0.686 and 0.650, respectively, $P \leq 0.05$). On the contrary, phospholipid metabolism significantly decreased comparing O versus H groups, suggesting a possible compensatory and/or adaptation mechanisms toward oxidative stress in PO subjects VAT. Phospholipids are amphipathic molecules containing both hydrophilic and hydrophobic moieties [27]. GPC and GPE are the most abundant phospholipids in mammals and provide the majority of cellular membrane lipids. Studies in muscle-specific CDP (ethanolaminephosphate cytidylyltransferase) knockout mice, an enzyme involved in GPE production, suggested that phospholipids, rather than diacylglycerol or triacylglycerol, are the probable modulators of muscle insulin resistance and obesity [28]. Maintaining a balance in the GPC : GPE ratio seems to be important for health; obesity and the concomitant oversupply of fatty acids divert this balance. Plasma lipidomic studies in humans have also shown a clear association between GPE (and consequently, a decreased GPG : GPE ratio) with obesity, pre-diabetes and type 2 diabetes mellitus [29,30]. This change was also observed in adipose tissue from PO and O subjects compared with H subjects (Table 6). Finally, the accumulation of lysolipids (Table 7) in PO tissues compared with obese (O) tissues, specifically 1-palmitoyl-GPC, 1-stearoyl-GPC, 1-palmitoyl-GPE, 1-stearoyl-GPE, 1-stearoyl-GPI and 1--stearoyl-GPS ($P < 0.05$), may highlight increased lipid membrane turnover in subjects with metabolic syndrome. The increases in lipid membrane turnover is not observed if we compare O and PO groups with the H group, suggesting that these metabolites are associated with obesity.

## Glucose-related metabolites

We also observed increased glucose levels in PO samples as well as higher levels of the isobaric compound mannitol/sorbitol and aminosugars, thus confirming the high levels of glucose and suggesting reduced glucose utilization or excess accumulation (Supplementary Table S2). Glucose metabolism has been found to be altered in obesity in both animal and human studies. Consistent with the development of type 2 diabetes in subjects with metabolic syndrome, there were significantly ($P < 0.05$) higher levels of glucose in the PO samples

Biochemical Journal (2018) **475** 1019–1035
https://doi.org/10.1042/BCJ20170604

**Table 6 Phospholipid and phosphatidylserine**

| Sub pathway | Biochemical name | Fold of change | | |
|---|---|---|---|---|
| | | O/H | PO/H | PO/O |
| Phospholipid metabolism | Choline | 0.8446 | 1.025 | 1.2135 |
| | Choline phosphate | 0.7411 | 0.927 | 1.2508 |
| | Cytidine 5'-diphosphocholine | 0.7675 | 0.7213 | 0.9398 |
| | Glycerophosphorylcholine (GPC) | 1.1283 | 1.3767 | 1.2202 |
| | Phosphoethanolamine | 0.6956 | 0.8006 | 1.151 |
| | Cytidine-5'-diphosphoethanolamine | 0.7169 | 0.7054 | 0.984 |
| | Glycerophosphoethanolamine | 0.7826 | 1.0496 | 1.3412 |
| | Trimethylamine *N*-oxide | 0.4647 | 0.5189 | 1.1166 |
| | Glycerophosphoinositol | 0.6834 | 0.6082 | 0.89 |
| | 1,2-dipalmitoyl-GPC (16:0/16:0) | 0.6984 | 0.921 | 1.3188 |
| | 1,2-dipalmitoyl-GPE (16:0/16:0) | 0.5557 | 0.7746 | 1.3938 |
| | 1-Palmitoyl-2-oleoyl-GPC (16:0/18:1) | 0.8633 | 1.0016 | 1.1602 |
| | 1-Palmitoyl-2-linoleoyl-GPC (16:0/18:2) | 0.8498 | 0.9106 | 1.0715 |
| | 1-Stearoyl-2-arachidonoyl-GPC (18:0/20:4) | 0.6342 | 0.9524 | 1.5016 |
| | 1-Stearoyl-2-oleoyl-GPC (18:0/18:1) | 0.7554 | 0.9112 | 1.2064 |
| | 1,2-Dioleoyl-GPC (18:1/18:1) | 0.7798 | 0.8107 | 1.0396 |
| | 1-Palmitoyl-2-arachidonoyl-GPC (16:0/20:4n6) | 0.693 | 0.8964 | 1.2936 |
| | 1-Stearoyl-2-linoleoyl-GPC (18:0/18:2) | 0.7834 | 0.9391 | 1.1987 |
| | 1-Palmitoyl-2-palmitoleoyl-GPC (16:0/16:1) | 1.0731 | 1.223 | 1.1397 |
| | 1-Stearoyl-2-arachidonoyl-GPI (18:0/20:4) | 0.8264 | 1.2414 | 1.5022 |
| | 1-Oleoyl-2-linoleoyl-GPC (18:1/18:2) | 0.7484 | 0.7876 | 1.0524 |
| | 1-Palmitoyl-2-arachidonoyl-GPI (16:0/20:4) | 0.9459 | 0.9118 | 0.964 |
| | 1-Palmitoyl-2-oleoyl-GPE (16:0/18:1) | 0.8476 | 0.906 | 1.0688 |
| | 1-Stearoyl-2-arachidonoyl-GPE (18:0/20:4) | 0.8252 | 1.0353 | 1.2546 |
| | 1-Stearoyl-2-oleoyl-GPE (18:0/18:1) | 0.856 | 1.0496 | 1.2262 |
| | 1-Palmitoyl-2-arachidonoyl-GPE (16:0/20:4) | 0.865 | 0.9296 | 1.0746 |
| | 1-Palmitoyl-2-linoleoyl-GPE (16:0/18:2) | 0.8183 | 0.753 | 0.9202 |
| | 1-Stearoyl-2-linoleoyl-GPE (18:0/18:2) | 0.8621 | 0.9628 | 1.1167 |
| | 1-Palmitoyl-2-stearoyl-GPC (16:0/18:0) | 0.5824 | 0.834 | 1.4319 |
| | 1,2-Dioleoyl-GPE (18:1/18:1) | 0.8626 | 0.9025 | 1.0462 |
| | 1-Stearoyl-2-oleoyl-GPG (18:0/18:1) | 0.7209 | 1.0062 | 1.3957 |
| | 1,2-Dilinoleoyl-GPC (18:2/18:2) | 0.6887 | 0.6175 | 0.8967 |
| | 1-Oleoyl-2-linoleoyl-GPE (18:1/18:2) | 0.7854 | 0.6868 | 0.8745 |
| | 1-Linoleoyl-2-arachidonoyl-GPC (18:2/20:4n6) | 0.5833 | 0.6506 | 1.1155 |
| | 1-Stearoyl-2-linoleoyl-GPS (18:0/18:2) | 0.8614 | 1.0575 | 1.2277 |
| | 1-Oleoyl-2-arachidonoyl-GPE (18:1/20:4) | 0.804 | 0.8962 | 1.1147 |
| | 1-Oleoyl-2-arachidonoyl-GPI (18:1/20:4) | 0.9686 | 0.9344 | 0.9647 |
| Phosphatidylserine (PS) | 1-Stearoyl-2-arachidonoyl-GPS (18:0/20:4) | 0.7531 | 1.0041 | 1.3333 |
| | 1-Stearoyl-2-oleoyl-GPS (18:0/18:1) | 0.722 | 0.9226 | 1.2778 |

Values in the table indicate ratio.
Green indicates significant differences ($P \leq 0.05$) between groups shown, metabolite ratio <1.00.
Red indicates significant differences ($P \leq 0.05$) between groups shown, metabolite ratio ≥1.00.
Non-colored: mean values are not significantly different for that comparison.

compared with O samples (Figure 5a,b); surprisingly, no significant differences were found comparing O *versus* H and PO *versus* H (Supplementary Table S2), and this could be probably due to biological variability between samples. No significant changes were found in TCA (tricarboxylic acid cycle) cycle (Supplementary Figure S2) intermediates, except for α-ketoglutarate, which was significantly increased in PO samples compared with O samples (fold change 1.678, $P < 0.05$). α-Ketoglutarate decreased comparing O *versus* H groups (fold change 0.518, $P < 0.05$) and PO *versus* H group, though the latter did not reached statistical significance (Supplementary Table S2). While not significant, the corresponding decrease in 1,5-anhydroglucitol (1,5-AG), the levels of which in blood are known to inversely mirror those of glucose due to their competition for clearance from the blood by the kidney [31], would be supportive of the elevated glucose levels (Figure 5a,b,e). While the focus of this study was adipose tissue, these changes along with a higher level of the isobaric

Biochemical Journal (2018) **475** 1019–1035
https://doi.org/10.1042/BCJ20170604

**Table 7 Lysolipid**

| Sub pathway | Biochemical name | Fold of change | | |
|---|---|---|---|---|
| | | O/H | PO/H | PO/O |
| Lysolipid | 1-Palmitoyl-GPC (16:0) | 0.5849 | 0.7111 | 1.2158 |
| | 2-Palmitoyl-GPC (16:0) | 0.6686 | 0.8627 | 1.2903 |
| | 1-Palmitoleoyl-GPC (16:1) | 0.4165 | 0.446 | 1.0709 |
| | 2-Palmitoleoyl-GPC (16:1) | 1.032 | 1.1464 | 1.1108 |
| | 1-Stearoyl-GPC (18:0) | 0.5739 | 0.7337 | 1.2784 |
| | 1-Oleoyl-GPC (18:1) | 0.5338 | 0.6243 | 1.1695 |
| | 1-Linoleoyl-GPC (18:2) | 0.6458 | 0.5818 | 0.901 |
| | 1-Arachidonoyl-GPC (20:4n6) | 0.7038 | 0.7937 | 1.1277 |
| | 1-Palmitoyl-GPE (16:0) | 0.5343 | 1.009 | 1.8884 |
| | 1-Stearoyl-GPE (18:0) | 0.6868 | 1.3916 | 2.0263 |
| | 1-Oleoyl-GPE (18:1) | 0.6491 | 0.9201 | 1.4176 |
| | 1-Linoleoyl-GPE (18:2) | 0.9047 | 0.604 | 0.6676 |
| | 1-Arachidonoyl-GPE (20:4n6) | 0.9047 | 1.0085 | 1.1148 |
| | 1-Stearoyl-GPI (18:0) | 0.6628 | 1.1757 | 1.7738 |
| | 1-Stearoyl-GPS (18:0) | 0.5028 | 1.0762 | 2.1403 |

Values in the table indicate ratio.
Green indicates significant differences ($P \leq 0.05$) between groups shown, metabolite ratio <1.00.
Red indicates significant differences ($P \leq 0.05$) between groups shown, metabolite ratio ≥1.00.
Non-colored: mean values are not significantly different for that comparison.

compound 2-hydroxybutyrate/2-hydroxyisobutyrate (Supplementary Table S2) are consistent with that of type 2 diabetes. In association with glucose, there were also trending ($0.05 < P < 0.10$) higher levels of the isobaric compound mannitol/sorbitol (Figure 5c,d), which may be an indication of excess glucose being shunted toward the sorbitol pathway and either reduced glucose utilization or excess accumulation. Additionally, there were also significantly higher levels of aminosugars (Figure 6a–e), including glucuronate and *N*-acetylglucosamine 6-phosphate ($0.05 < P < 0.10$, trend toward a significant difference), and *N*-acetylglucosamine 1-phosphate, *N*-acetylneuraminate and erythronate ($P < 0.05$), which may also be indicative of increased glucose levels.

# Discussion

Obesity dramatically increases the risk of developing metabolic, cardiovascular and oncological diseases, and poses a heavy burden to society [32,33]. Specifically, VAT has a crucial role in the development of some of the most important obesity-related comorbidities, including insulin resistance, type 2 diabetes, dyslipidemia, hypertension and nonalcoholic fatty liver disease. The excess fat that is unable to be stored in adipose tissue tends to accumulate in other tissues, including the liver and muscle, causing toxic effects related to the excessive accumulation of reactive lipid species [34–39]. The accumulation of fat in the muscle and liver tends to worsen insulin resistance resulting in alterations in lipid and carbohydrate metabolism. Insulin resistance, and the consequent hyperinsulinemia, plays a central role in the alterations of many metabolic pathways, including protein synthesis, uptake of glucose in muscle and adipose tissue, proteolysis, lipid metabolism, glycogen metabolism and endogenous glucose production [40]. The data reported here demonstrate that in VAT collected from obese individuals with metabolic syndrome (PO) compared with metabolically healthy obese individuals (O) and nonobese healthy controls (H), significant differences can be observed. Focusing on PO versus O groups, we observed dysregulation of oxidative stress markers, multiple lipid metabolic pathways and increased markers of elevated glucose levels. Obesity decreases antioxidant defenses by lowering several antioxidant enzymes, including glutathione peroxidase, glutathione reductase and catalase, and by altering the activity of cytochrome P450 [41,42]. In agreement with this perspective, we found high levels of GSSG, cysteine-glutathione disulfide, methionine sulfone, *N*-acetylmethionine sulfoxide and cysteine, supporting the hypothesis of altered redox homeostasis and increased oxidative stress in adipose tissue extracted from PO subjects compared with H subjects. Another relevant result is the dysregulation of multiple lipid metabolic pathways, which contribute to the onset and progression of metabolic disease. Specifically, we confirmed the role of ceramides in the metabolic

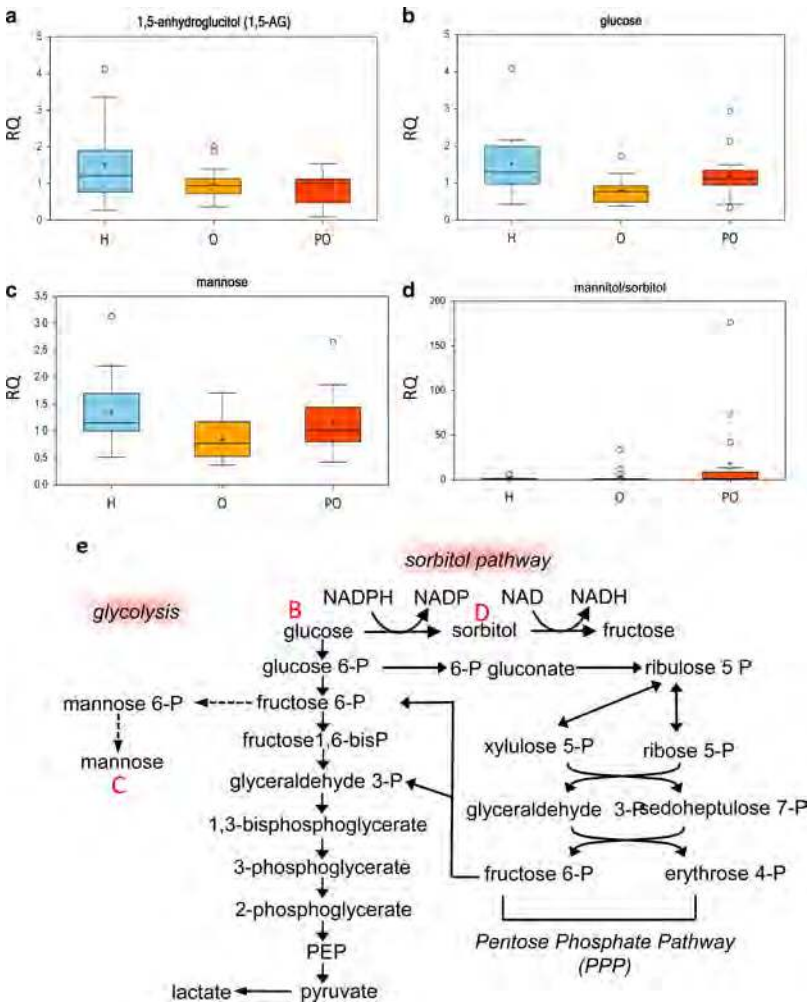


**Figure 5. Glucose-related metabolites are modulated in obese and pathologically obese adipose tissue.**

The levels of anhydroglucitol(1,5-AG) (**a**), glucose (**b**), mannose (**c**) and mannitol/sorbitol (**d**) were differentially detected in pathologically obese adipose tissue versus obese tissues. Pathway connections of the cited metabolites are shown in (**e**). The box legend is as indicated in Figure 2I. H, healthy; O, obese; PO, pathologically obese. Data have been plotted in the whisker plots. Detailed statistics are shown in Supplementary Table S2.

complications of obesity; ceramide is generated in response to obesity signals [such as saturated fatty acids, lipopolysaccharide or proinflammatory stimuli by enhancement of sphingolipid biosynthesis or sphingolipid recycling) [43–45]. There are several studies suggesting that specific sphingolipids may provide a common pathway that links excess nutrients and inflammation to increased metabolic and cardiovascular risk [46,47]. Moreover, ceramides antagonize insulin signaling at the level of RACα serine/threonine-protein kinase [48,49], and their actions can be resolved from those of glucosylceramides. Inhibition or ablation of the enzymes that catalyze the formation of ceramides causes insulin sensitization, anti-artherogenic properties and cardioprotection [46,50–53]. In addition, consistent with the literature linking ceramides with inflammation, we observed high levels of 15-HETE and prostaglandins in subjects with PO compared with the O group. Another interesting finding from our study is the altered levels of sphingomyelins in the adipose tissue of PO subjects, as other studies have suggested the role of sphingomyelins containing saturated, but not unsaturated, acyl-chains in the obesity, insulin resistance and decreased liver function in young adults with obesity [54,55]. Our findings agree with the genetic ablation of the *Sgms2* gene in mice which reduces plasma membrane levels of sphingomyelin and inhibits weight gain, while also increasing glucose tolerance and insulin sensitivity in animals fed a high-fat diet compared with wild-type controls [36,56].

Biochemical Journal (2018) **475** 1019–1035
https://doi.org/10.1042/BCJ20170604

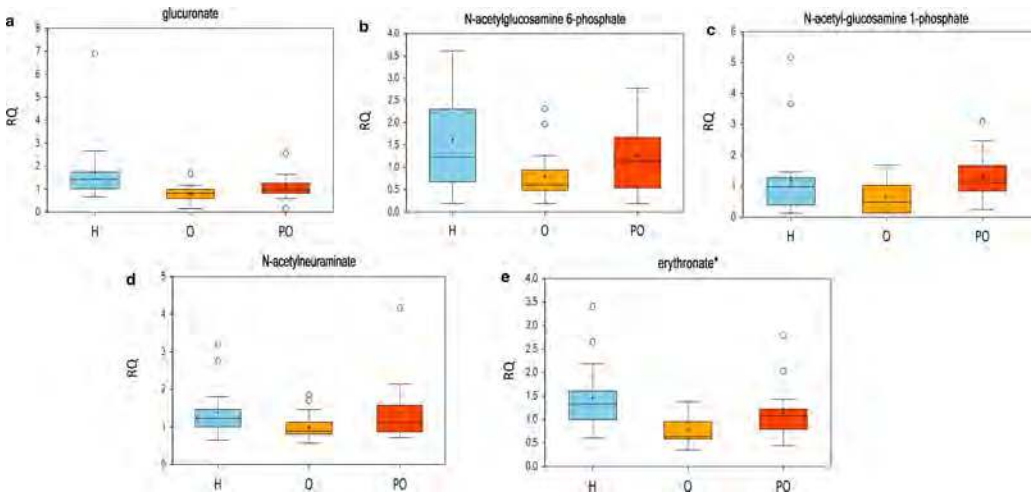


**Figure 6. Accumulation of aminosugars in pathologically obese tissue.**

The accumulation of aminosugars indicates abnormal glucose metabolism. Gluconate (**a**), *N*-acetylglucosamine 6-phosphate (**b**), *N*-acetylglucosamine 1-phosphate (**c**), *N*-acetylneuraminate (**d**) and erythronate (**e**) were increased in pathologically obese tissues versus obese tissues. The box legend is as indicated in Figure 2l. H, healthy; O, obese; PO, pathologically obese. Data have been plotted in the whisker plots. Detailed statistics are shown in Supplementary Table S2.

We also found a significantly greater number of detected plasmalogens in the PO samples compared with those from H and O subjects. Again, our data implicate a relevant role for plasmalogens in PO subjects. These are a class of phospholipids that are expressed in many human tissues. They are important structural components of membranes and appear to play an important role not only in diseases such as obesity, type 2 diabetes and inflammation but also in cancer and heart failure [57]. Plasmalogens have antioxidant and anti-inflammatory activity and protect unsaturated lipid membranes from oxidative products. Recent studies suggest that plasmalogens can modulate oxidative stress, inflammation and cholesterol efflux in the setting of metabolic disease [58,59]. Some conflicting data in the literature on plasmalogens in various metabolic diseases could be explained by the fact that plasmalogen levels increase as a compensatory response to the development of metabolic syndrome [58]. The role of plasmalogens in diabetes mellitus has been outlined in recent years. In type 1 diabetes, they were found to be consistently diminished in the serum of children who later progressed to T1D, while proinflammatory LPCs were elevated in the serum several months before autoantibodies could be detected [60]. A possible explanation for this might be that β-cells are particularly susceptible to oxidative stress [61] and that plasmalogens can serve as radical scavengers. In patients with end-stage renal disease, plasmalogens represent a marker of oxidative stress and are simultaneously depleted in erythrocyte membranes and predictive of cardiovascular mortality [62].

Surprisingly, we found that some metabolic pathways, including the one related to oxidative stress, phospholipid metabolism, plasmalogens and sphingolipids metabolism, were not significantly affected comparing PO versus H groups, while did not significantly change or significantly decreased comparing O versus H groups. Taking into account the complexity of the data obtained, we cannot explain why the PO group shares common metabolomic signature with the H group. We cannot exclude that the biological variability within datasets limited the statistical significance and hence the biochemical interpretation of the present study. Note that adipose tissue, especially from obese and nonobese individuals, may be dramatically different between groups due to many factors including reduced levels of cytoplasmic levels within cells due to intracellular lipids. Taking into account all the limitations of the present study, we limited our attention to specific metabolites that significantly changed among the groups.

# Conclusion

Limited metabolic differences were observed within this dataset comparing samples collected from pathologically obese, healthy obese patients and healthy lean subjects. RF analysis was able to effectively segregate the O from the H samples. While there were limited differences between the PO and O patient-derived samples, we

found consistent indications of increased oxidative stress markers from the PO samples in addition to increased markers of elevated glucose levels, findings which may be consistent with metabolic syndrome. In the adipose tissue derived from the PO subjects, there were significantly elevated levels of plasmalogens. Ceramides and sphingolipids were also increased, which may reflect changes in cellular signaling or sphingolipid turnover. The GPC : GPE ratio was altered in PO samples.

The collection of additional patient's tissue specimens to increase the power of the study to limit individual biological variability as well as the combined analysis of additional matrices (i.e. plasma) will be necessary in future work to increase the rigorous aspect of the present study. Nevertheless, our data show that in the adipose tissue of patients with metabolic syndrome, there were many biochemical alterations that confirm the theory that increased adipose tissue mass induces a chronic inflammatory state and oxidative stress. The results obtained will possibly serve as preliminary data to develop new hypothesis and innovative targeted therapies.

## Abbreviations

1,5-AG, 1,5-anhydroglucitol; 15-HETE, 15-hydroxyeicosatetraenoic acid; BMI, body mass index; ESI, electrospray ionization; FA, fatty acids; GGT, gamma-glutamyl transferase; GPC, glycerolphosphorylcholine; GPE, glycerolphosphorylethanolamine; GPI, glycerolphosphorylinositol; GPS, glycerolphosphorylserine; GSH, glutathione; GSSG, oxidized glutathione; HDL, high-density lipoprotein; LPC, lysophosphatidylcholine; PO, pathologically obese; RF, random forest; RP, reverse phase; VAT, visceral adipose tissue.

## Author Contribution

E.C. and M.T. wrote the article and prepared figures and tables. A.M.L. and M.A.-P. prepared samples for MS analysis. P.G. and G.S. have performed the surgery. C.C., F.S., V.R. and G.R. evaluated the clinical features, managed the database and collected samples. N.D.D. and G.M. interpreted the results.

## Funding

This work was mainly supported by 'Fondazione Roma' NCD (to G.M., E.C., N.D.D. and M.T.), partially supported by Ministero Sanita (IDI-IRCCS R.C. to G.M. and E.C.) and MAECI (CN18GR09 to G.M.).

## Competing Interests

The Authors declare that there are no competing interests associated with the manuscript.

## References

1 Chen, Q., Shou, P., Zheng, C., Jiang, M., Cao, G., Yang, Q. et al. (2016) Fate decision of mesenchymal stem cells: adipocytes or osteoblasts? *Cell Death Differ.* **23**, 1128–1139 https://doi.org/10.1038/cdd.2015.168

2 Daquinag, A.C., Tseng, C., Salameh, A., Zhang, Y., Amaya-Manzanares, F., Dadbin, A. et al. (2015) Depletion of white adipocyte progenitors induces beige adipocyte differentiation and suppresses obesity development. *Cell Death Differ.* **22**, 351–363 https://doi.org/10.1038/cdd.2014.148

3 Machado, M.V., Michelotti, G.A., Jewell, M.L., Pereira, T.A., Xie, G., Premont, R.T. et al. (2016) Caspase-2 promotes obesity, the metabolic syndrome and nonalcoholic fatty liver disease. *Cell Death Dis.* **7**, e2096 https://doi.org/10.1038/cddis.2016.19

4 Park, H.S., Ju, U.I., Park, J.W., Song, J.Y., Shin, D.H., Lee, K.H. et al. (2016) PPARgamma neddylation essential for adipogenesis is a potential target for treating obesity. *Cell Death Differ.* **23**, 1296–1311 https://doi.org/10.1038/cdd.2016.6

5 Pitocco, D., Tesauro, M., Alessandro, R., Ghirlanda, G. and Cardillo, C. (2013) Oxidative stress in diabetes: implications for vascular and other complications. *Int. J. Mol. Sci.* **14**, 21525–21550 https://doi.org/10.3390/ijms141121525

6 Zheng, C., Yang, Q., Cao, J., Xie, N., Liu, K., Shou, P. et al. (2016) Local proliferation initiates macrophage accumulation in adipose tissue during obesity. *Cell Death Dis.* **7**, e2167 https://doi.org/10.1038/cddis.2016.54

7 Savini, I., Catani, M.V., Evangelista, D., Gasperi, V. and Avigliano, L. (2013) Obesity-associated oxidative stress: strategies finalized to improve redox state. *Int. J. Mol. Sci.* **21**, 10497–10538 https://doi.org/10.3390/ijms140510497

8 Fridlyand, L.E. and Philipson, L.H. (2006) Reactive species and early manifestation of insulin resistance in type 2 diabetes. *Diabetes Obes. Metab.* **8**, 136–145 https://doi.org/10.1111/j.1463-1326.2005.00496.x

9 Houstis, N., Rosen, E.D. and Lander, E.S. (2006) Reactive oxygen species have a causal role in multiple forms of insulin resistance. *Nature* **440**, 944–948 https://doi.org/10.1038/nature04634

10 Lisak, D., Schacht, T., Gawlitza, A., Albrecht, P., Aktas, O., Koop, B. et al. (2016) BAX inhibitor-1 is a $Ca^{2+}$ channel critically important for immune cell function and survival. *Cell Death Differ.* **23**, 358–368 https://doi.org/10.1038/cdd.2015.115

11 Campia, U., Tesauro, M. and Cardillo, C. (2012) Human obesity and endothelium-dependent responsiveness. *Br. J. Pharmacol.* **165**, 561–573 https://doi.org/10.1111/j.1476-5381.2011.01661.x

12 Chen, S.Z., Ning, L.F., Xu, X., Jiang, W.Y., Xing, C., Jia, W.P. et al. (2016) The miR-181d-regulated metalloproteinase Adamts1 enzymatically impairs adipogenesis via ECM remodeling. *Cell Death Differ.* **23**, 1778–1791 https://doi.org/10.1038/cdd.2016.66

13 Schaffer, S.W., Jong, C.J. and Mozaffari, M. (2012) Role of oxidative stress in diabetes-mediated vascular dysfunction: unifying hypothesis of diabetes revisited. *Vascul. Pharmacol.* **57**, 139–149 https://doi.org/10.1016/j.vph.2012.03.005

Biochemical Journal (2018) **475** 1019–1035
https://doi.org/10.1042/BCJ20170604


14 Tesauro, M. and Cardillo, C. (2011) Obesity, blood vessels and metabolic syndrome. *Acta Physiol.* **203**, 279–286 https://doi.org/10.1111/j.1748-1716.2011.02290.x

15 Schaffer, S.W., Jong, C.J. and Mozaffari, M. (2012) Role of oxidative stress in diabetes-mediated vascular dysfunction: unifying hypothesis of diabetes revisited. *Vascul. Pharmacol.* **57**, 139–149 https://doi.org/10.1016/j.vph.2012.03.005

16 Cunha, D.A., Cito, M., Carlsson, P.O., Vanderwinden, J.M., Molkentin, J.D., Bugliani, M. et al. (2016) Thrombospondin 1 protects pancreatic beta-cells from lipotoxicity via the PERK-NRF2 pathway. *Cell Death Differ.* **23**, 1995–2006 https://doi.org/10.1038/cdd.2016.89

17 Huo, J., Ma, Y., Liu, J.J., Ho, Y.S., Liu, S., Soh, L.Y. et al. (2016) Loss of Fas apoptosis inhibitory molecule leads to spontaneous obesity and hepatosteatosis. *Cell Death Dis.* **7**, e2091 https://doi.org/10.1038/cddis.2016.12

18 Qatanani, M. and Lazar, M.A. (2007) Mechanisms of obesity-associated insulin resistance: many choices on the menu. *Genes Dev.* **21**, 1443–1455 https://doi.org/10.1101/gad.1550907

19 Lopategi, A., López-Vicario, C., Alcaraz-Quiles, J., García-Alonso, V., Rius, B., Titos, E. et al. (2016) Role of bioactive lipid mediators in obese adipose tissue inflammation and endocrine dysfunction. *Mol. Cell. Endocrinol.* **419**, 44–59 https://doi.org/10.1016/j.mce.2015.09.033

20 Després, J.P. and Lemieux, I. (2006) Abdominal obesity and metabolic syndrome. *Nature* **444**, 881–887 https://doi.org/10.1038/nature05488

21 Nedungadi, T.P. and Clegg, D.J. (2009) Sexual dimorphism in body fat distribution and risk for cardiovascular diseases. *J. Cardiovasc. Transl. Res.* **2**, 321–327 https://doi.org/10.1007/s12265-009-9101-1

22 Schinzari, F., Tesauro, M. and Cardillo, C. (2017) Endothelial and perivascular adipose tissue abnormalities in obesity-related vascular dysfunction: novel targets for treatment. *J. Cardiovasc. Pharmacol.* **69**, 360–368 https://doi.org/10.1097/FJC.0000000000000469

23 Grundy, S.M., Brewer, Jr, H.B., Cleeman, J.I., Smith, Jr, S.C. and Lenfant, C. (2004) Definition of metabolic syndrome: report of the National Heart, Lung, and Blood Institute/American Heart Association conference on scientific issues related to definition. *Circulation* **109**, 433–438 https://doi.org/10.1161/01.CIR.0000111245.75752.C6

24 Aburasayn, H., Al Batran, R. and Ussher, J.R. (2016) Targeting ceramide metabolism in obesity. *Am. J. Physiol. Endocrinol. Metab.* **311**, E423–E435 https://doi.org/10.1152/ajpendo.00133.2016

25 Wallner, S. and Schmitz, G. (2011) Plasmalogens the neglected regulatory and scavenging lipid species. *Chem. Phys. Lipids* **164**, 573–589 https://doi.org/10.1016/j.chemphyslip.2011.06.008

26 Mathis, D. and Shoelson, S.E. (2011) Immunometabolism: an emerging frontier. *Nat. Rev. Immunol.* **11**, 81 https://doi.org/10.1038/nri2922

27 Balsinde, J., Balboa, M.A. and Dennis, E.A. (1997) Inflammatory activation of arachidonic acid signaling in murine P388D1 macrophages via sphingomyelin synthesis. *J. Biol. Chem.* **272**, 20373–20377 https://doi.org/10.1074/jbc.272.33.20373

28 Selathurai, A., Kowalski, G.M., Burch, M.L., Sepulveda, P., Risis, S., Lee-Young, R.S. et al. (2015) The CDP-ethanolamine pathway regulates skeletal muscle diacylglycerol content and mitochondrial biogenesis without altering insulin sensitivity. *Cell Metab.* **21**, 718–730 https://doi.org/10.1016/j.cmet.2015.04.001

29 Meikle, P.J., Wong, G., Barlow, C.K., Weir, J.M., Greeve, M.A., MacIntosh, G.L. et al. (2013) Plasma lipid profiling shows similar associations with prediabetes and type 2 diabetes. *PLoS ONE* **8**, e74341 https://doi.org/10.1371/journal.pone.0074341

30 Weir, J.M., Wong, G., Barlow, C.K., Greeve, M.A., Kowalczyk, A., Almasy, L. et al. (2013) Plasma lipid profiling in a large population-based cohort. *J. Lipid Res.* **54**, 2898–2908 https://doi.org/10.1194/jlr.P035808

31 Buse, J.B., Freeman, J.L., Edelman, S.V., Jovanovic, L. and McGill, J.B. (2003) Serum 1,5-anhydroglucitol (GlycoMark): a short-term glycemic marker. *Diabetes Technol. Ther.* **5**, 355–363 https://doi.org/10.1089/152091503765691839

32 Iantorno, M., Campia, U., Di Daniele, N., Nistico, S., Forleo, G.B., Cardillo, C. et al. (2014) Obesity, inflammation and endothelial dysfunction. *J. Biol. Regul. Homeost. Agents* **28**, 169–176 PMID:25001649

33 Poloz, Y. and Stambolic, V. (2015) Obesity and cancer: a case for insulin signaling. *Cell Death Dis.* **6**, e2037 https://doi.org/10.1038/cddis.2015.381

34 Cohen, J.C., Horton, J.D. and Hobbs, H.H. (2011) Human fatty liver disease: old questions and new insights. *Science* **332**, 1519–1523 https://doi.org/10.1126/science.1204265

35 Kotronen, A. and Yki-Jarvinen, H. (2008) Fatty liver: a novel component of the metabolic syndrome. *Arterioscler. Thromb. Vasc. Biol.* **28**, 27–38 https://doi.org/10.1161/ATVBAHA.107.147538

36 Liu, Z., Gan, L., Wu, T., Feng, F., Luo, D., Gu, H. et al. (2016) Adiponectin reduces ER stress-induced apoptosis through PPARalpha transcriptional regulation of ATF2 in mouse adipose. *Cell Death Dis.* **7**, e2487 https://doi.org/10.1038/cddis.2016.388

37 Magtanong, L., Ko, P.J. and Dixon, S.J. (2016) Emerging roles for lipids in non-apoptotic cell death. *Cell Death Differ.* **23**, 1099–1109 https://doi.org/10.1038/cdd.2016.25

38 Wang, Y.T., Chiang, H.H., Huang, Y.S., Hsu, C.L., Yang, P.J., Juan, H.F. et al. (2016) A link between adipogenesis and innate immunity: RNase-L promotes 3T3-L1 adipogenesis by destabilizing Pref-1 mRNA. *Cell Death Dis.* **7**, e2458 https://doi.org/10.1038/cddis.2016.323

39 Zoller, V., Funcke, J.B., Keuper, M., Abd El Hay, M., Debatin, K.M., Wabitsch, M. et al. (2016) TRAIL (TNF-related apoptosis-inducing ligand) inhibits human adipocyte differentiation via caspase-mediated downregulation of adipogenic transcription factors. *Cell Death Dis.* **7**, e2412 https://doi.org/10.1038/cddis.2016.286

40 Wilcox, G. (2005) Insulin and insulin resistance. *Clin. Biochem. Rev.* **26**, 19–39 PMID:16278749

41 Ozaydin, A., Onaran, I., Yesim, T.E., Sargin, H., Avsar, K. and Sultuybek, G. (2006) Increased glutathione conjugate transport: a possible compensatory protection mechanism against oxidative stress in obesity? *Int. J. Obes.* **30**, 134–140 https://doi.org/10.1038/sj.ijo.0803108

42 Tangvarasittichai, S. (2015) Oxidative stress, insulin resistance, dyslipidemia and type 2 diabetes mellitus. *World J. Diabetes* **6**, 456–480 https://doi.org/10.4239/wjd.v6.i3.456

43 Bagnati, M., Ogunkolade, B.W., Marshall, C., Tucci, C., Hanna, K., Jones, T.A. et al. (2016) Glucolipotoxicity initiates pancreatic beta-cell death through TNFR5/CD40-mediated STAT1 and NF-κB activation. *Cell Death Dis.* **7**, e2329 https://doi.org/10.1038/cddis.2016.203

44 Maceyka, M. and Spiegel, S. (2014) Sphingolipid metabolites in inflammatory disease. *Nature* **510**, 58–67 https://doi.org/10.1038/nature13475

45 Qi, D., Tang, X., He, J., Wang, D., Zhao, Y., Deng, W. et al. (2016) Omentin protects against LPS-induced ARDS through suppressing pulmonary inflammation and promoting endothelial barrier via an Akt/eNOS-dependent mechanism. *Cell Death Dis.* **7**, e2360 https://doi.org/10.1038/cddis.2016.265

46 Jiang, X.C., Goldberg, I.J. and Park, T.S. (2011) Sphingolipids and cardiovascular diseases: lipoprotein metabolism, atherosclerosis and cardiomyopathy. *Adv. Exp. Med. Biol.* **721**, 19–39 https://doi.org/10.1007/978-1-4614-0650-1_2
47 Porta, C., Subhra Kumar, B., Larghi, P., Rubino, L., Mancino, A. and Sica, A. (2007) Tumor promotion by tumor-associated macrophages. *Adv. Exp. Med. Biol.* **604**, 67–86. https://doi.org/10.1007/978-0-387-69116-9_5
48 Cavallo, M.G., Pozzilli, P., Bird, C., Wadhwa, M., Meager, A., Visalli, N. et al. (1991) Cytokines in sera from insulin-dependent diabetic patients at diagnosis. *Clin. Exp. Immunol.* **86**, 256–259 https://doi.org/10.1111/j.1365-2249.1991.tb05806.x
49 Mishima, Y., Kuyama, A., Tada, A., Takahashi, K., Ishioka, T. and Kibata, M. (2001) Relationship between serum tumor necrosis factor-alpha and insulin resistance in obese men with type 2 diabetes mellitus. *Diabetes Res. Clin. Pract.* **52**, 119–123 https://doi.org/10.1016/S0168-8227(00)00247-3
50 Chaurasia, B. and Summers, S.A. (2015) Ceramides–lipotoxic inducers of metabolic disorders. *Trends Endocrinol. Metab.* **26**, 538–550 https://doi.org/10.1016/j.tem.2015.07.006
51 Garufi, A., Trisciuoglio, D., Cirone, M. and D'Orazi, G. (2016) Zncl2 sustains the Adriamycin-induced cell death inhibited by high glucose. *Cell Death Dis.* **7**, e2280 https://doi.org/10.1038/cddis.2016.178
52 Hojjati, M.R., Li, Z., Zhou, H., Tang, S., Huan, C., Ooi, E. et al. (2005) Effect of myriocin on plasma sphingolipid metabolism and atherosclerosis in apoE-deficient mice. *J. Biol. Chem.* **280**, 10284–10289 https://doi.org/10.1074/jbc.M412348200
53 Holland, W.L., Brozinick, J.T., Wang, L.P., Hawkins, E.D., Sargent, K.M., Liu, Y. et al. (2007) Inhibition of ceramide synthesis ameliorates glucocorticoid-, saturated-fat-, and obesity-induced insulin resistance. *Cell Metab.* **5**, 167–179 https://doi.org/10.1016/j.cmet.2007.01.002
54 Bai, Y., Shang, Q., Zhao, H., Pan, Z., Guo, C., Zhang, L. et al. (2016) Pdcd4 restrains the self-renewal and white-to-beige transdifferentiation of adipose-derived stem cells. *Cell Death Dis.* **7**, e2169 https://doi.org/10.1038/cddis.2016.75
55 Hanamatsu, H., Ohnishi, S., Sakai, S., Yuyama, K., Mitsutake, S., Takeda, H. et al. (2014) Altered levels of serum sphingomyelin and ceramide containing distinct acyl chains in young obese adults. *Nutr. Diabetes* **4**, e141 https://doi.org/10.1038/nutd.2014.38
56 Sugimoto, M., Shimizu, Y., Zhao, S., Ukon, N., Nishijima, K., Wakabayashi, M. et al. (2016) Characterization of the role of sphingomyelin synthase 2 in glucose metabolism in whole-body and peripheral tissues in mice. *Biochim. Biophys. Acta* **1861**, 688–702 https://doi.org/10.1016/j.bbalip.2016.04.019
57 Gorgas, K., Teigler, A., Komljenovic, D. and Just, W.W. (2006) The ether lipid-deficient mouse: tracking down plasmalogen functions. *Biochim. Biophys. Acta* **1763**, 1511–1526 https://doi.org/10.1016/j.bbamcr.2006.08.038
58 Scarfe, G.B., Wright, B., Clayton, E., Taylor, S., Wilson, I.D., Lindon, J.C. et al. (1998) 19F-NMR and directly coupled HPLC-NMR-MS investigations into the metabolism of 2-bromo-4-trifluoromethylaniline in rat: a urinary excretion balance study without the use of radiolabelling. *Xenobiotica* **28**, 373–388 https://doi.org/10.1080/004982598239489
59 Meikle, P.J. and Summers, S.A. (2017) Sphingolipids and phospholipids in insulin resistance and related metabolic disorders. *Nat. Rev. Endocrinol.* **13**, 79–91 https://doi.org/10.1038/nrendo.2016.169
60 Orešič, M., Simell, S., Sysi-Aho, M., Näntö-Salonen, K., Seppänen-Laakso, T., Parikka, V. et al. (2008) Dysregulation of lipid and amino acid metabolism precedes islet autoimmunity in children who later progress to type 1 diabetes. *J. Exp. Med.* **205**, 2975–2984 https://doi.org/10.1084/jem.20081800
61 Lenzen, S., Drinkgern, J. and Tiedge, M. (1996) Low antioxidant enzyme gene expression in pancreatic islets compared with various other mouse tissues. *Free Radic. Biol. Med.* **20**, 463–466 https://doi.org/10.1016/0891-5849(96)02051-5
62 Stenvinkel, P., Diczfalusy, U., Lindholm, B. and Heimburger, O. (2004) Phospholipid plasmalogen, a surrogate marker of oxidative stress, is associated with increased cardiovascular mortality in patients on renal replacement therapy. *Nephrol. Dial. Transplant.* **19**, 972–976 https://doi.org/10.1093/ndt/gfh035

# Supplementary Materials and Methods

## Study Parameters

Data Quality and Instrument and Process Variability:

| *QC Sample* | *Measurement* | *Median RSD* |
|---|---|---|
| Internal Standards | Instrument Variability | 4 % |
| Endogenous Biochemicals | Total Process Variability | 8 % |

Instrument variability was determined by calculating the median relative standard deviation (RSD) for the internal standards that were added to each sample prior to injection into the mass spectrometers. Overall process variability was determined by calculating the median RSD for all endogenous metabolites (i.e., non-instrument standards) present in 100% of the Client Matrix samples, which are technical replicates of pooled client samples. Values for instrument and process variability as shown in the table above meet Metabolon's acceptance criteria.

## Metabolon Platform

**Sample Accessioning:** Following receipt, samples were inventoried and immediately stored at -80$^{o}$C. Each sample received was accessioned into the Metabolon LIMS system and was assigned by the LIMS a unique identifier that was associated with the original source identifier only. This identifier was used to track all sample handling, tasks, results, etc. The samples (and all derived aliquots) were tracked by the LIMS system. All portions of any sample were automatically assigned their own unique identifiers by the LIMS when a new task was created; the relationship of these samples was also tracked. All samples were maintained at -80$^{o}$C until processed.

**QA/QC:** Several types of controls were analyzed in concert with the experimental samples: a pooled matrix sample generated by taking a small volume of each experimental sample (or alternatively, use of a pool of well-characterized human plasma) served as a technical replicate throughout the data set; extracted water samples served as process blanks; and a cocktail of QC standards that were carefully chosen not to interfere with the measurement of endogenous compounds were spiked into every analyzed sample, allowed instrument performance monitoring and aided chromatographic alignment. Tables 1 and 2 (shown on the following page) describe these QC samples and standards. Instrument variability was determined by calculating the median relative standard deviation (RSD) for the standards that were added to each sample prior to injection into the mass spectrometers. Overall process variability was determined by calculating the median RSD for all endogenous metabolites (i.e., non-instrument standards) present in 100% of the pooled matrix samples. Experimental samples were randomized across the platform run with QC samples spaced evenly among the injections, as outlined in Figure 1, on the following page.

**Table 1: Description of Metabolon QC Samples**

| Type | Description | Purpose |
|---|---|---|
| MTRX | Large pool of human plasma maintained by Metabolon that has been characterized extensively. | Assure that all aspects of the Metabolon process are operating within specifications. |
| CMTRX | Pool created by taking a small aliquot from every customer sample. | Assess the effect of a non-plasma matrix on the Metabolon process and distinguish biological variability from process variability. |
| PRCS | Aliquot of ultra-pure water | Process Blank used to assess the contribution to compound signals from the process. |
| SOLV | Aliquot of solvents used in extraction. | Solvent Blank used to segregate contamination sources in the extraction. |

**Table 2: Metabolon QC Standards**

| Type | Description | Purpose |
|---|---|---|
| RS | Recovery Standard | Assess variability and verify performance of extraction and instrumentation. |
| IS | Internal Standard | Assess variability and performance of instrument. |

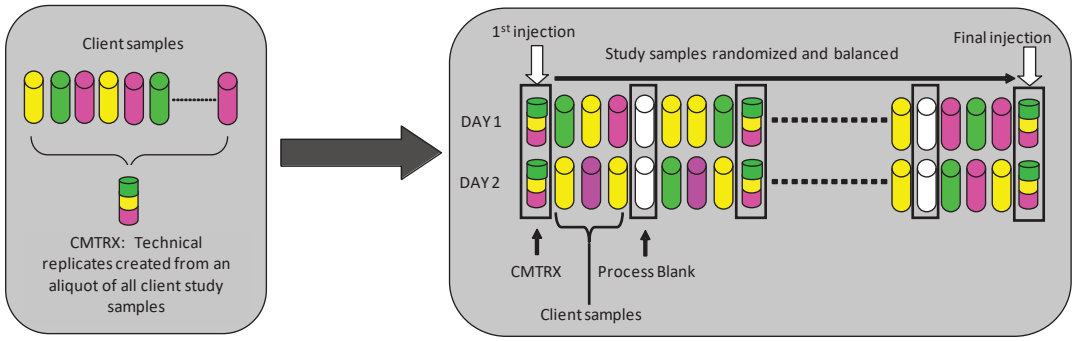


**Figure 1. Preparation of client-specific technical replicates.** A small aliquot of each client sample (colored cylinders) is pooled to create a CMTRX technical replicate sample (multi-colored cylinder), which is then injected periodically throughout the platform run. Variability among consistently detected biochemicals can be used to calculate an estimate of overall process and platform variability.

**Ultrahigh Performance Liquid Chromatography-Tandem Mass Spectroscopy (UPLC-MS/MS):** All methods utilized a Waters ACQUITY ultra-performance liquid chromatography (UPLC) and a Thermo Scientific Q-Exactive high resolution/accurate mass spectrometer interfaced with a heated electrospray ionization (HESI-II) source and Orbitrap mass analyzer operated at 35,000 mass resolution. The sample extract was dried then reconstituted in solvents compatible to each of the four methods. Each reconstitution solvent contained a series of standards at fixed concentrations to ensure injection and chromatographic consistency. One aliquot was analyzed using acidic positive ion conditions, chromatographically optimized for more hydrophilic compounds. In this method, the extract was gradient eluted from a C18 column (Waters UPLC BEH C18-2.1x100 mm, 1.7 µm) using water and methanol, containing 0.05% perfluoropentanoic acid (PFPA) and 0.1% formic acid (FA). Another aliquot was also analyzed using acidic positive ion conditions, however it was chromatographically optimized for more hydrophobic compounds. In this method, the extract was gradient eluted from the same afore mentioned C18 column using methanol, acetonitrile, water, 0.05% PFPA and 0.01% FA and was operated at an overall higher organic content. Another aliquot was analyzed using basic negative ion optimized conditions using a separate dedicated C18 column. The basic extracts were gradient eluted from the column using methanol and water, however with 6.5mM Ammonium Bicarbonate at pH 8. The fourth aliquot was analyzed via negative ionization following elution from a HILIC column (Waters UPLC BEH Amide 2.1x150 mm, 1.7 µm) using a gradient consisting of water and acetonitrile with 10mM Ammonium Formate, pH 10.8. The MS analysis alternated between MS and data-dependent $MS^n$ scans using dynamic exclusion. The scan range varied slighted between methods but covered 70-1000 m/z. Raw data files are archived and extracted as described below.

**Bioinformatics:** The informatics system consisted of four major components, the Laboratory Information Management System (LIMS), the data extraction and peak-identification software, data processing tools for QC and compound identification, and a collection of information interpretation and visualization tools for use by data analysts. The hardware and software foundations for these informatics components were the LAN backbone, and a database server running Oracle 10.2.0.1 Enterprise Edition.

**LIMS:** The purpose of the Metabolon LIMS system was to enable fully auditable laboratory automation through a secure, easy to use, and highly specialized system. The scope of the Metabolon LIMS system encompasses sample accessioning, sample preparation and instrumental analysis and reporting and advanced data analysis. All of the subsequent software systems are grounded in the LIMS data structures. It has been modified to leverage and interface with the in-house information extraction and data visualization systems, as well as third party instrumentation and data analysis software.

**Data Extraction and Compound Identification:** Raw data was extracted, peak-identified and QC processed using Metabolon's hardware and software. These systems are built on a web-service platform utilizing Microsoft's .NET technologies, which run on high-performance application servers and fiber-channel storage arrays in clusters to provide active failover and load-balancing. Compounds were identified by comparison to library entries of purified standards or recurrent unknown entities. Metabolon maintains a library based on authenticated standards that contains the retention time/index (RI), mass to charge ratio (*m/z)*, and chromatographic data (including MS/MS spectral data) on all molecules present in the library. Furthermore, biochemical identifications are based on three criteria: retention index within a narrow RI window of the proposed identification, accurate mass match to the library +/- 10 ppm, and the MS/MS forward and reverse scores between the experimental

data and authentic standards. The MS/MS scores are based on a comparison of the ions present in the experimental spectrum to the ions present in the library spectrum. While there may be similarities between these molecules based on one of these factors, the use of all three data points can be utilized to distinguish and differentiate biochemicals. More than 3300 commercially available purified standard compounds have been acquired and registered into LIMS for analysis on all platforms for determination of their analytical characteristics. Additional mass spectral entries have been created for structurally unnamed biochemicals, which have been identified by virtue of their recurrent nature (both chromatographic and mass spectral). These compounds have the potential to be identified by future acquisition of a matching purified standard or by classical structural analysis.

**Curation:** A variety of curation procedures were carried out to ensure that a high quality data set was made available for statistical analysis and data interpretation. The QC and curation processes were designed to ensure accurate and consistent identification of true chemical entities, and to remove those representing system artifacts, mis-assignments, and background noise. Metabolon data analysts use proprietary visualization and interpretation software to confirm the consistency of peak identification among the various samples. Library matches for each compound were checked for each sample and corrected if necessary.

**Metabolite Quantification and Data Normalization:** Peaks were quantified using area-under-the-curve. For studies spanning multiple days, a data normalization step was performed to correct variation resulting from instrument inter-day tuning differences. Essentially, each compound was corrected in run-day blocks by registering the medians to equal one (1.00) and normalizing each data point proportionately (termed the "block correction"; Figure 2). For studies that did not require more than one day of analysis, no normalization is necessary, other than for purposes of data visualization. In certain instances, biochemical data may have been normalized to an additional factor (e.g., cell counts, total protein as determined by Bradford assay, osmolality, etc.) to account for differences in metabolite levels due to differences in the amount of material present in each sample.

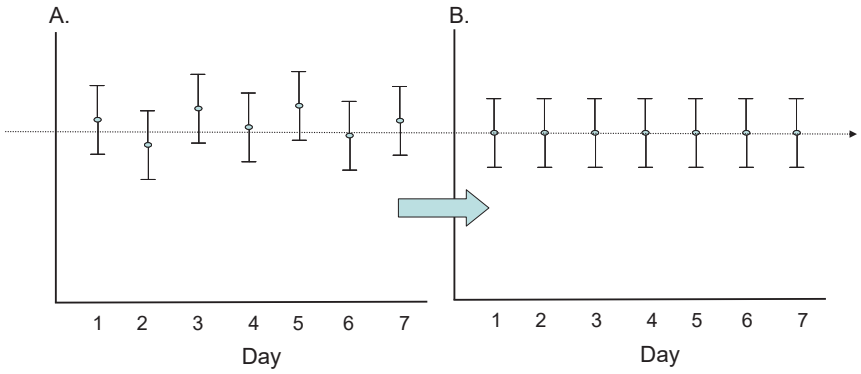


**Figure 2: Visualization of data normalization steps for a multiday platform run.**

## Statistical Methods and Terminology

**Statistical Calculations:** For many studies, two types of statistical analysis are usually performed: (1) significance tests and (2) classification analysis. Standard statistical analyses are performed in ArrayStudio on log transformed data. For those analyses not standard in ArrayStudio, the programs R (http://cran.r-project.org/) or JMP are used. Below are examples of frequently employed significance tests and classification methods followed by a discussion of p- and q-value significance thresholds.

1. **Welch's two-sample *t*-test**

   Welch's two-sample *t*-test is used to test whether two unknown means are different from two independent populations.

   This version of the two-sample *t*-test allows for unequal variances (variance is the square of the standard deviation) and has an *approximate t*-distribution with degrees of freedom estimated using Satterthwaite's approximation. The test statistic is given by $t = (\bar{x}_1 - \bar{x}_2)/\sqrt{s_1^2/n_1 + s_2^2/n_2}$, and the degrees of freedom is given by $\left(\frac{s_1^2}{n_1} + \frac{s_2^2}{n_2}\right)^2 / \left(\frac{\left(\frac{s_1^2}{n_1}\right)^2}{n_1 - 1} + \frac{\left(\frac{s_2^2}{n_2}\right)^2}{n_2 - 1}\right)$, where $\bar{x}_1, \bar{x}_2$ are the sample means, $s_1$, $s_2$, are the sample standard deviations, and $n_1$, $n_2$ are the samples sizes from groups 1 and 2, respectively. We typically use a two-sided test (tests whether the means are different) as opposed to a one-sided test (tests whether one mean is greater than the other).

2. **Matched Pairs *t*-test**

   The matched pairs *t*-test is used to test whether two unknown means are different from paired observations taken on the same subjects.

   The matched pairs *t*-test is equivalent to the one-sample *t*-test performed on the differences of the observations taken on each subject (i.e., calculate $(x_1 - x_2)$ for each subject; test whether the mean difference is zero or not). The test statistic is given by $t = (\bar{x}_1 - \bar{x}_2)/n$, with $n - 1$ degrees of freedom, where $\bar{x}_1, \bar{x}_2$ are the sample means for groups 1 and 2, respectively, $s_d$ is the standard deviation of the differences, $n$ is the number of *subjects* (so there are $2n$ observations).

3. **One-way ANOVA**

   ANOVA stands for analysis of variance. For ANOVA, it is assumed that all populations have the same variances. One-way ANOVA is used to test whether at least two unknown means are all equal or whether at least one pair of means is different. For the case of two means, ANOVA gives the same result as a two-sided *t*-test with a pooled estimate of the variance.

   An ANOVA uses an F-test which has two parameters – the numerator degrees of freedom and the denominator degrees of freedom. The degrees of freedom in the numerator are equal to $g - 1$, where $g$ is the number of groups. If $n$ is the total number of observations ($n_1 + n_2$), then, the denominator degrees of freedom is equal to $n - g$. The F-statistic is the ratio of the between-groups variance to the within-groups

variance, hence the higher the F-statistic the more evidence we have that the means are different.

Often within ANOVA, one performs linear contrasts for specific comparisons of interest. For example, suppose we have three groups A, B, C, then examples of some contrasts are A vs. B, the average of A and B vs. C, etc. For single-degree of freedom contrasts, these give the same result as a two-sided *t*-test with the pooled estimate of the variance from the ANOVA and degrees of freedom $n - g$. Below, we show the three formulas for A vs. B from a three group design as shown above. The numerator is same in each case, but the denominator differs by the estimates of the variances, and the degrees of freedom are different for each (if the theoretical assumptions hold, then the contrast has the most power, as it has the largest degrees of freedom).

Welch's two-sample *t*-test

By $t = (\bar{x}_A - \bar{x}_B)/\sqrt{s_A^2/n_A + s_B^2/n_B}$ , and the degrees of freedom is given by $\left(\frac{s_A^2}{n_A} + \frac{s_B^2}{n_B}\right)^2 / \left( \frac{\left(\frac{s_A^2}{n_A}\right)^2}{n_A - 1} + \frac{\left(\frac{s_B^2}{n_B}\right)^2}{n_B - 1} \right)$

Two-sample *t*-test with pooled estimate of variance from A and B

$$t = (\bar{x}_A - \bar{x}_B)/\sqrt{s_{AB}^2(1/n_A + /n_B)}$$

where $s_{AB}^2 = \left((n_A - 1)s_A^2 + (n_B - 1)s_B^2\right)/(n_A + n_B - 2)$, where the degrees of freedom is $n_A + n_B - 2$.

The contrast from the ANOVA,

$$t = (\bar{x}_A - \bar{x}_B)/\sqrt{s^2(1/n_A + /n_B)}$$

where $s^2 = \left((n_A - 1)s_A^2 + (n_B - 1)s_B^2 + (n_C - 1)s_C^2\right)/(n_A + n_B + n_C - 3)$, where the degrees of freedom is given by where the degrees of freedom is $n_A + n_B + n_C - 3$.

## 4. Two-way ANOVA

ANOVA stands for analysis of variance. For ANOVA, it is assumed that all populations have the same variances. For a two-way ANOVA, three statistical tests are typically performed: the main effect of each factor and the interaction. Suppose we have two factors A and B, where A represent the genotype and B represent the diet in a mouse study. Suppose each of these factors has two levels (A: wild type, knock out; B: standard diet, high fat diet). For this example, there are 4 combinations ("treatments"): A1B1, A1B2, A2B1, A2B2. The overall ANOVA F-test gives the p-value for testing whether all four of these means are equal or whether at least one pair is different. However, we are also interested in the effect of the genotype and diet. A main effect is a contrast that tests one factor across the levels of the other factor. Hence the A main effect compares (A1B1 + A1B2)/2 vs. (A2B1 + A2B2)/2, and the B-main effect compares (A1B1 + A2B2)/2 vs. (A1B2 + A2B2)/2. The interaction is a contrast that tests whether the mean difference for one factor depends on the level of the other factor, which is (A1B2 + A2B1)/2 vs. (A1B1 + A2B2)/2.

Some sample plots follow. For the first plot, there is a B main effect, but no A main effect and no interaction, as the effect of B does not depend on the level of A. For the second plot, notice how the mean difference for B is the same at each level of A and the difference in A is the same for each level of B, hence there is no statistical interaction. The final plot also has main effects for A and B, but here also has an interaction: we see the effect of B depends on the level of A (0 for A1 but 2 for A2), i.e., the effect of the diet depends on the genotype. We also see here the interpretation of the main effects depends on whether there is an interaction or not.

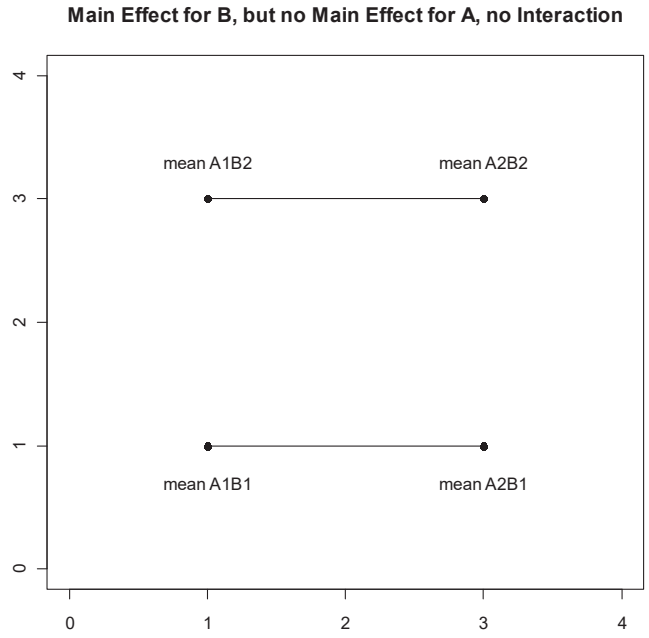

**Main Effect for A, Main Effect for B, No Interaction**

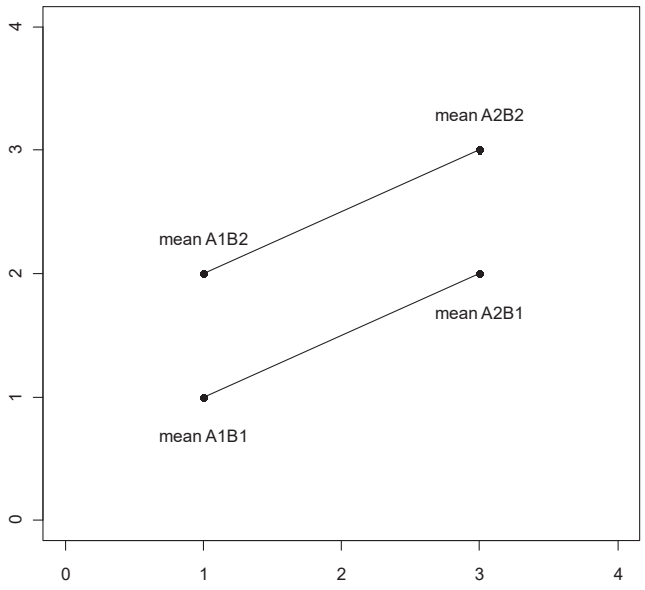


**Main Effect for A, Main Effect for B, with Interaction**

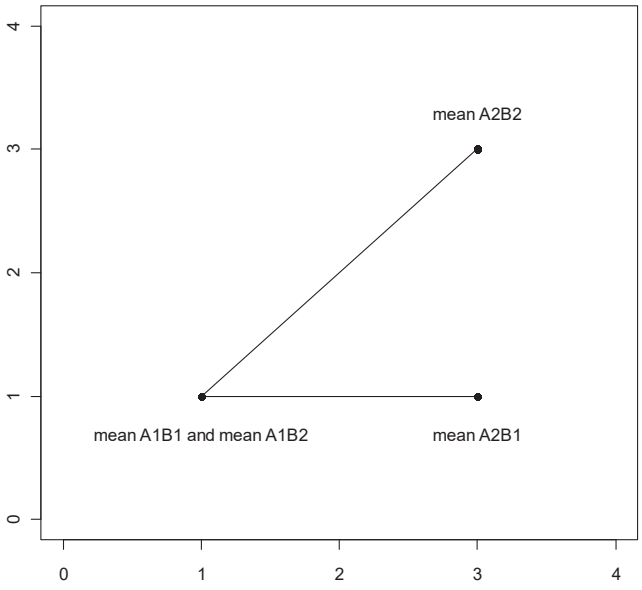

5. **Two-way Repeated Measures ANOVA**

This is typically an ANOVA where one factor is applied to each subject and the second factor is a time point. See two-way ANOVA as many of the details are similar except that the model takes into account the repeated measures, i.e., the treatments are given to the same subject over time. The two main effects and the interaction are assessed, with particular interest to the interaction, as this shows where the time profiles are parallel or not for the treatments (parallel mean no interaction).

One additional note, the standard analysis assumes a condition referred to as compound symmetry, which assumes the correlation between each pair of levels of the repeated-measures factor is the same. Thus, for the case of time, it assumes the correlation is the same between time points 1 and 2, 1 and 3, and 2 and 3.

6. **Correlation**

Correlation measures the strength and direction of a *linear* association between two variables. The statistical test for correlation tests whether the true correlation is zero or not.

The square of the correlation is the percentage of the total variation explained by a linear relationship between the two variables. Thus, with large sample sizes there may be a sample correlation of 0.1 that is statistically significant. This means we have high confidence that the true correlation is zero, however, only 100*(0.1*0.1)% = 1% of the variation of one variable is explained by a linear relationship with the other variable, so while there is an association, it has little predictive ability.

7. **Hotelling's $T^2$ test**

The Hotelling's $T^2$ test is a multivariate generalization of the *t*-test, but here we are testing whether the mean vectors are different or not (the vector consists of multiple metabolites).

The Hotelling statistic is: $t^2 = \left(\frac{n_x n_y}{n_x+n_y}\right) * (\overline{\boldsymbol{x}} - \overline{\boldsymbol{y}})^T \boldsymbol{S}^{-1} (\overline{\boldsymbol{x}} - \overline{\boldsymbol{y}})$, where $n_x$ and $n_y$ are the numbers of samples in each group, $\overline{\boldsymbol{x}}$ is the mean vector of the variables from group 1, $\overline{\boldsymbol{y}}$ is the mean vector of variables from group 2 and $\mathbf{S}$ is the pooled estimate of the variance-covariance matrix of the variables. This analysis assumes the underlying variance-covariance matrix is the same for each group. Notice that in the case of uncorrelated variables, this is simply a weighted average of the squared mean differences with weights inversely proportional to the sample variances (i.e., the metabolites less variable within a group are given higher weights).

## 8. p-values

For statistical significance testing, p-values are given. The lower the p-value, the more evidence we have that the null hypothesis (typically that two population means are equal) is not true. If "statistical significance" is declared for p-values less than 0.05, then 5% of the time we incorrectly conclude the means are different, when actually they are the same.

The p-value is the probability that the test statistic is at least as extreme as observed in this experiment given that the null hypothesis is true. Hence, the more extreme the statistic, the lower the p-value and the more evidence the data gives against the null hypothesis.

## 9. q-values

The level of 0.05 is the false positive rate when there is one test. However, for a large number of tests we need to account for false positives. There are different methods to correct for multiple testing. The oldest methods are family-wise error rate adjustments (Bonferroni, Tukey, etc.), but these tend to be extremely conservative for a very large number of tests. With gene arrays, using the False Discovery Rate (FDR) is more common. The family-wise error rate adjustments give one a high degree of confidence that there are zero false discoveries. However, with FDR methods, one can allow for a small number of false discoveries. The FDR for a given set of compounds can be estimated using the q-value (see Storey J and Tibshirani R. (2003) Statistical significance for genomewide studies. Proc. Natl. Acad. Sci. USA 100: 9440-9445; PMID: 12883005).

In order to interpret the q-value, the data must first be sorted by the p-value then choose the cutoff for significance (typically $p<0.05$). The q-value gives the false discovery rate for the selected list (i.e., an estimate of the proportion of false discoveries for the list of compounds whose p-value is below the cutoff for significance). For Table 1 below, if the whole list is declared significant, then the false discovery rate is approximately 10%. If everything from Compound 079 and above is declared significant, then the false discovery rate is approximately 2.5%.

Table 1: Example of q-value interpretation

| Compound | *p*-value | *q*-value |
|---|---|---|
| Compound 103 | 0.0002 | 0.0122 |
| Compound 212 | 0.0004 | 0.0122 |
| Compound 076 | 0.0004 | 0.0122 |
| Compound 002 | 0.0005 | 0.0122 |
| Compound 168 | 0.0006 | 0.0122 |
| Compound 079 | 0.0016 | 0.0258 |
| Compound 113 | 0.0052 | 0.0631 |
| Compound 050 | 0.0053 | 0.0631 |
| Compound 098 | 0.0061 | 0.0647 |
| Compound 267 | 0.0098 | 0.0939 |

## 10. Random Forest

Random forest is a supervised classification technique based on an ensemble of decision trees (see Breiman L. (2001) Random Forests. Machine Learning. 45: 5-32; http://link.springer.com/article/10.1023%2FA%3A1010933404324). For a given decision tree, a random subset of the data with identifying true class information is selected to build the tree ("bootstrap sample" or "training set"), and then the remaining data, the "out-of-bag" (OOB) variables, are passed down the tree to obtain a class prediction for each sample. This process is repeated thousands of times to produce the forest. The final classification of each sample is determined by computing the class prediction frequency ("votes") for the OOB variables over the whole forest. For example, suppose the random forest consists of 50,000 trees and that 25,000 trees had a prediction for sample 1. Of these 25,000, suppose 15,000 trees classified the sample as belonging to Group A and the remaining 10,000 classified it as belonging to Group B. Then the votes are 0.6 for Group A and 0.4 for Group B, and hence the final classification is Group A. This method is unbiased since the prediction for each sample is based on trees built from a subset of samples that do not include that sample. When the full forest is grown, the class predictions are compared to the true classes, generating the "OOB error rate" as a measure of prediction accuracy. Thus, the prediction accuracy is an unbiased estimate of how well one can predict sample class in a new data set. Random forest has several advantages – it makes no parametric assumptions, variable selection is not needed, it does not overfit, it is invariant to transformation, and it is fairly easy to implement with R.

To determine which variables (biochemicals) make the largest contribution to the classification, a "variable importance" measure is computed. We use the "Mean Decrease Accuracy" (MDA) as this metric. The MDA is determined by randomly permuting a variable, running the observed values through the trees, and then reassessing the prediction accuracy. If a variable is not important, then this procedure will have little change in the accuracy of the class prediction (permuting random noise will give random noise). By contrast, if a variable is important to the classification, the prediction accuracy will drop after such a permutation, which we record as the MDA. Thus, the random forest analysis provides an "importance" rank ordering of biochemicals; we typically output the top 30 biochemicals in the list as potentially worthy of further investigation.

## 11. Hierarchical Clustering

Hierarchical clustering is an unsupervised method for clustering the data, and can show large-scale differences. There are several types of hierarchical clustering and many distance metrics that can be used. A common method is complete clustering using the Euclidean distance, where each sample is a vector with all of the metabolite values. The differences seen in the cluster may be unrelated to the treatment groups or study design.

## 12. Principal Components Analysis (PCA)

Principal components analysis is an unsupervised analysis that reduces the dimension of the data. Each principal component is a linear combination of every metabolite and the principal components are uncorrelated. The number of principal components is equal to the number of observations.

The first principal component is computed by determining the coefficients of the metabolites that maximizes the variance of the linear combination. The second component finds the coefficients that maximize the variance with the condition that the second component is orthogonal to the first. The third component is orthogonal to the first two components and so on. The total variance is defined as the sum of the variances of the predicted values of each component (the variance is the square of the standard deviation), and for each component, the proportion of the total variance is computed. For example, if the standard deviation of the predicted values of the first principal component is 0.4 and the total variance = 1, then 100*0.4*0.4/1 = 16% of the total variance is explained by the first component. Since this is an unsupervised method, the main components may be unrelated to the treatment groups, and the "separation" does not give an estimate of the true predictive ability.

## 13. Z-scores

An intensity measurement for a metabolite by itself does not tell much. If for example a patient contains a blood glucose level of 300, this could be very good news if most people have blood glucose levels around 300, but less so if most people have levels around 100. In other words a measurement is meaningful only relative to the means of the sample or the population. This can be achieved by transforming the measurements into Z-scores which are expressed as standard deviations from the mean.

The Z-score, also called the standard score or normal score, is a dimensionless quantity derived by subtracting the control population mean from an individual raw score and then dividing the difference by the control population standard deviation. The Z-score indicates how many standard deviations an observation is above or below the mean of the control group. The Z-score is negative when the raw score is below the mean, positive when above. Since knowing the true mean and standard deviation of a control population is often unrealistic, the mean and standard deviation of the control population may be estimated using a random control sample.

Z-score = $\frac{x - \mu}{\sigma}$

where: x is a raw score to be standardized, μ is the mean of the control population, σ is the standard deviation of the control population

Subtracting the mean *centers* the distribution, and dividing by the standard deviation *standardizes* the distribution. The interesting properties of Z-scores are that they have a zero mean (effect of "centering") and a variance and standard deviation of 1 (effect of "standardizing"). This is because all distributions expressed in Z-scores have the same mean (0) and the same variance (1), so we can use Z-scores to compare observations coming from different distributions. When a distribution is normal most of the Z-scores (more than 99%) lay between the values of -3 and +3

## Obese versus Healthy

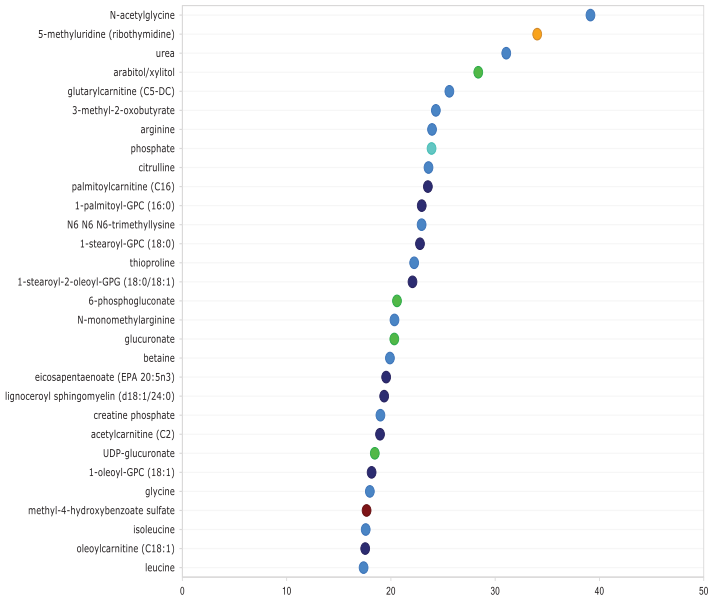


**Random Forest Confusion Matrix**

Predicted Group

| Actual Group | Healthy | Obese | Class Error |
|---|---|---|---|
| Healthy | 12 | 5 | 0.2941 |
| Obese | 5 | 13 | 0..2778 |
| Predictive accuracy = 71% | | | |

- Amino Acid
- Carbohydrate
- Energy
- Lipid
- Nucleotide
- Xenobiotics

## Healthy versus Pathological Obese

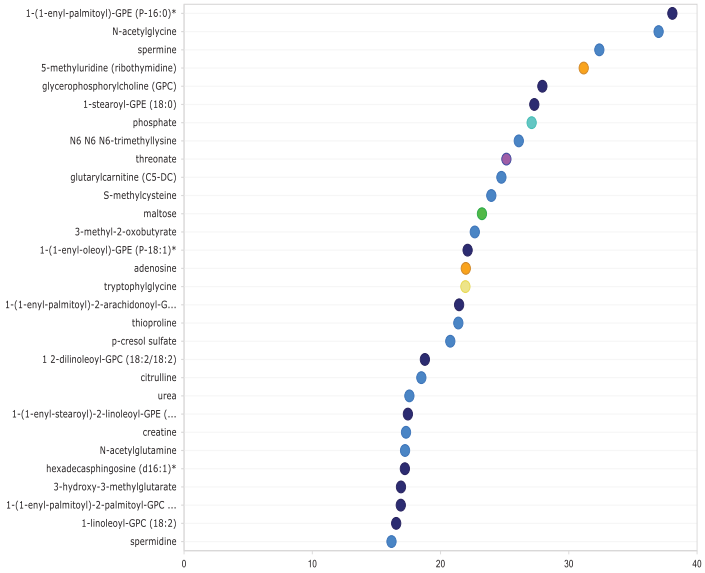


**Random Forest Confusion Matrix**

Predicted Group

| Actual Group | Healthy | P obese | Class Error |
|---|---|---|---|
| Healthy | 12 | 5 | 0.2941 |
| P obese | 2 | 16 | 0.1111 |
| Predictive accuracy = 80% | | | |

- Amino Acid
- Carbohydrate
- Cofactors and Vitamins
- Energy
- Lipid
- Nucleotide
- Peptide

## Obese versus Pathological Obese

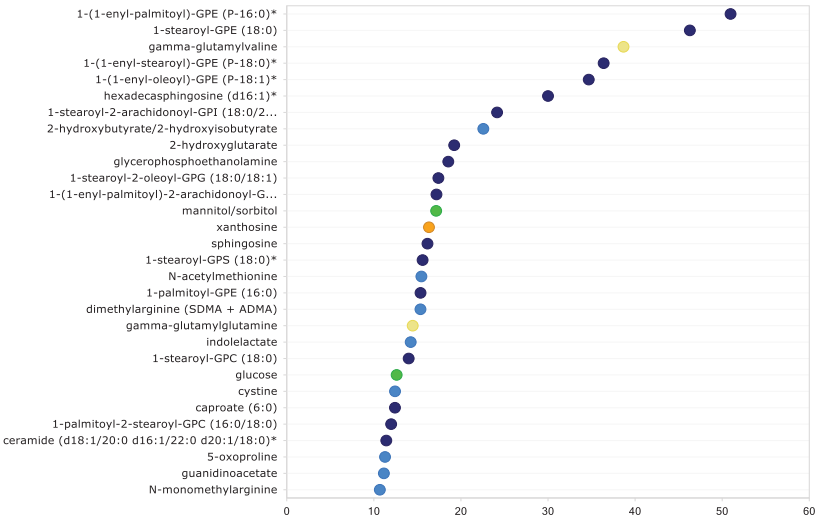


**Random Forest Confusion Matrix**

Predicted Group

| Actual Group | obese | P obese | Class Error |
|---|---|---|---|
| obese | 13 | 5 | 0.2778 |
| P obese | 6 | 12 | 0.3333 |
| Predictive accuracy = 69% | | | |

- Amino Acid
- Carbohydrate
- Lipid
- Nucleotide
- Peptide

Increasing Importance to Group Separation

mean-decrease-accuracy

**Fig S1**

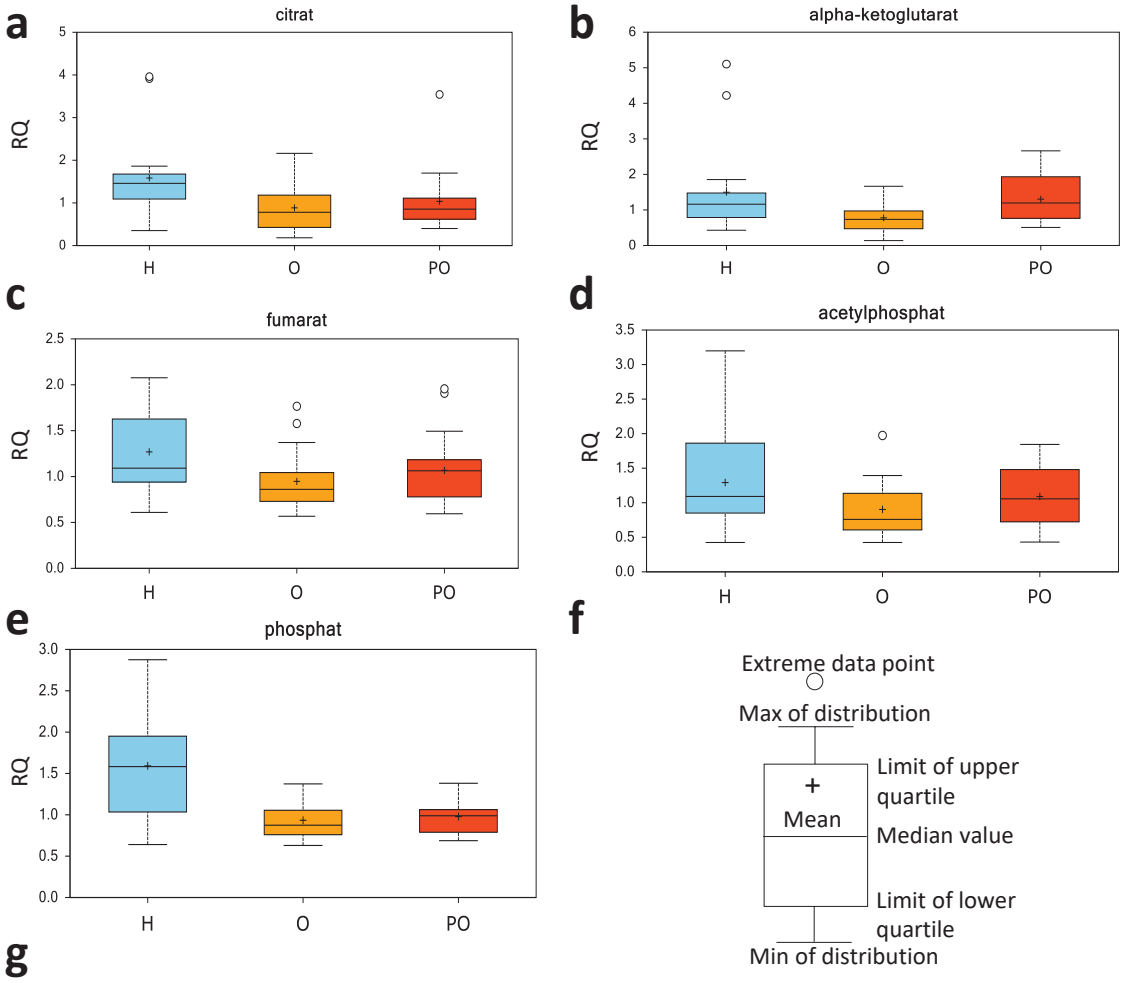
a
citrat
RQ
H
O
PO
b
alpha-ketoglutarat
c
fumarat
d
acetylphosphat
e
phosphat
f
Extreme data point
Max of distribution
Limit of upper quartile
Mean
Median value
Limit of lower quartile
Min of distribution
g
TCA cycle
pyruvate
LDH
PDH
FA synthesis
acetyl-CoA
CS
citrate
A
aconitase
oxaloacetate
cis-aconitate
MDH
NADH
NAD+
malate
isocitrate
fumarase
aspartate
phenylalanine
tyrosine
NAD+
NADH
IDH1
fumarate
C
α-ketoglutarate
glutaminolysis
FADH2
FAD
SDH
NAD+
B
2-hydroxyglutarate
NADH
succinate
succinyl-CoA
isoleucine & valine
branched-chain amino acids
succinyl-CoA synthetase

**Fig S2**

## Supplementary Figure Legends

**Figure S1. Groups separation by Random Forest analysis.** Analysis shows a moderate ability to segregate Obese from the Healthy controls while segregation between Obese and Pathological Obese was less prevalent.

**Figure S2. Tricarboxylic acid cycle and oxidative phosphate metabolites are not modulated in obese and patological obese adipose tissue.** Levels of citrate (**a**), fumarate (**b**), acetylphosphate (**c**) and phosphate (**d**) were not differentially modulated in pathological obese adipose tissue in comparison to obese tissues. Instead, $\alpha$-ketoglutarate levels were significantly ($p<0.05$) increased in PO in comparison with O samples. The box legend is shown in (**f**). Pathways connection of the cited metabolites are shown in (**g**). H, healthy; O, obese, PO, pathological obese. PDH: Pyruvate dehydrogenase; LDH: Lactate dehydrogenase; CS: Citrate synthase; IDH1: Isocitrate dehydrogenase 1; SCH: Succinate dehydrogenase; MDH: Malate dehydrogenase.

## SUPPLEMENTARY TABLE 1: CLINICAL DATA OF THE PATIENTS INVESTIGATED

| SAMPLES | DATE OF SAMPLE | DATE OF BIRTH | GENDER | WEIGHT | HEIGHT | BMI | WAIST | MAP | BP-SIS | BP-DIA | GLYCATED HEMOGLOBIN | GLYCEMIA | TOTAL CHOLESTEROL | LDL CHOLESTEROL | HDL CHOLESTEROL | TRIGLYCERIDES |
|---|---|---|---|---|---|---|---|---|---|---|---|---|---|---|---|---|
| **Healthy subjects (group 1: H)** | | | | | | | | | | | | | | | | |
| **A7** | ######## | 11/7/1981 | M | 65 | 1.75 | 21.22 | 89 | 86.6667 | 120 | 70 | 28 | 76 | 180 | 120 | 40 | 100 |
| **A8** | ######## | 7/29/1957 | F | 55 | 1.6 | 21.48 | 81 | 103.333 | 140 | 85 | 40 | 88 | 185 | 105 | 38 | 120 |
| **A9** | ######## | 2/17/1958 | F | 70 | 1.55 | 29.13 | 86 | 96.6667 | 130 | 80 | 37 | 76 | 190 | 95 | 69 | 132 |
| **A11** | ######## | 3/15/1946 | F | 60 | 1.55 | 24.97 | 84 | 106.667 | 140 | 90 | 38 | 84 | 223 | 124 | 76 | 173 |
| **A12** | 5/6/2015 | 9/2/1954 | F | 68 | 1.6 | 26.56 | 84 | 86.6667 | 110 | 75 | 39 | 89 | 180 | 119 | 37 | 140 |
| **A13** | ######## | 5/16/1951 | M | 60 | 1.78 | 18.93 | 87 | 101.667 | 135 | 85 | 40 | 86 | 175 | 117 | 33 | 127 |
| **A 14** | ######## | 8/23/1945 | F | 75 | 1.6 | 29.29 | 86 | 98.3333 | 125 | 85 | 36 | 82 | 185 | 127 | 35 | 110 |
| **A 15** | ######## | ######### | M | 82 | 1.8 | 25.3 | 94 | 100 | 140 | 80 | 38 | 87 | 170 | 116 | 36 | 100 |
| **A 16** | ######## | 2/14/1989 | F | 77 | 1.75 | 25.15 | 80 | 86.6667 | 120 | 70 | 23 | 92 | 189 | 117 | 62 | 51 |
| **A17** | 6/8/2015 | 12/5/1982 | F | 88 | 1.73 | 29.4 | 84 | 95 | 125 | 80 | 38 | 88 | 190 | 123 | 45 | 112 |
| **A18** | 6/8/2015 | 1/1/1964 | F | 86 | 1.72 | 29.06 | 86 | 93.3333 | 130 | 75 | 34 | 95 | 180 | 118 | 41 | 97 |
| **A 20** | ######## | 7/10/1971 | M | 70 | 1.78 | 22.09 | 92 | 98.3333 | 135 | 80 | 35 | 101 | 190 | 140 | 37 | 115 |
| **A2** | ######## | 6/26/1971 | F | 71 | 1.56 | 29.17 | 84 | 90 | 120 | 75 | 38 | 82 | 212 | 121 | 77 | 70 |
| **A3** | ######## | ######### | F | 50 | 1.65 | 18.36 | 78 | 101.667 | 125 | 90 | 33 | 70 | 168 | 104 | 54 | 52 |
| **A4** | ######## | 7/20/1943 | F | 72 | 1.7 | 24.91 | 82 | 106.667 | 140 | 90 | 39 | 90 | 198 | 140 | 37 | 110 |
| **A5** | ######## | 1/20/1957 | M | 75 | 1.7 | 25.95 | 92 | 98.3333 | 135 | 80 | 36 | 75 | 141 | 85 | 36 | 102 |
| **A6** | ######## | 7/22/1958 | M | 90 | 1.75 | 29.38 | 97 | 91.6667 | 115 | 80 | 40 | 87 | 170 | 114 | 37 | 113 |
| **MEAN** | | | | 71.412 | 1.681 | 25.315 | 86.2353 | 96.5686 | 128.5294 | 80.588 | 36 | 85.1765 | 183.8824 | 116.7647 | 46.47059 | 107.2941176 |
| **STANDARD DEVIATION** | | | | 2.7441 | 0.021 | 0.911 | 1.24714 | 1.60085 | 2.299485 | 1.5389 | 1.10147 | 1.89666 | 4.398264 | 3.377618 | 3.661322 | 7.309725947 |
| **Obese subjects without METs (group 2: O)** | | | | | | | | | | | | | | | | |
| **B6** | ######## | 5/3/1976 | F | 140 | 1.68 | 49.6 | 114 | 98.3333 | 125 | 85 | 39 | 85 | 233 | 152 | 53 | 142 |
| **B8** | ######## | 2/14/1968 | F | 150 | 1.68 | 53.14 | 118 | 106.667 | 140 | 90 | 36 | 85 | 168 | 98 | 58 | 60 |
| **B9** | ######## | 5/7/1975 | F | 128 | 1.75 | 41.79 | 106 | 100 | 130 | 85 | 40 | 93 | 190 | 113 | 61 | 78 |
| **B10** | ######## | 4/21/1987 | F | 104 | 1.68 | 36.84 | 98 | 86.6667 | 120 | 70 | 28 | 82 | 214 | 117 | 75 | 113 |
| **B11** | ######## | 3/21/1995 | F | 155 | 1.73 | 51.78 | 114 | 90 | 120 | 75 | 40 | 89 | 242 | 148 | 44 | 250 |
| **B12** | 6/8/2015 | 1/23/1963 | F | 120 | 1.66 | 43.54 | 108 | 91.6667 | 135 | 70 | 39 | 84 | 226 | 60 | 48 | 84 |
| **B13** | 6/8/2015 | ######### | F | 130 | 1.65 | 47.75 | 111 | 100 | 130 | 85 | 40 | 85 | 160 | 97 | 43 | 103 |
| **B14** | 7/9/2015 | 4/14/1970 | M | 170 | 1.8 | 52.46 | 117 | 113.333 | 150 | 95 | 36 | 80 | 174 | 115 | 48 | 98 |
| **B15** | ######## | 8/6/1968 | M | 150 | 1.73 | 50.11 | 116 | 96.6667 | 130 | 80 | 33 | 93 | 213 | 141 | 52 | 100 |
| **B16** | 9/8/2015 | 1/30/1958 | M | 100 | 1.78 | 31.56 | 106 | 93.3333 | 130 | 75 | 35 | 107 | 180 | 116 | 50 | 120 |
| **B17** | ######## | 8/1/1954 | F | 105 | 1.68 | 37.2 | 100 | 83.3333 | 110 | 70 | 37 | 105 | 185 | 123 | 48 | 118 |
| **B18** | ######## | ######### | F | 95 | 1.55 | 39.54 | 105 | 93.3333 | 120 | 80 | 36 | 67 | 129 | 107 | 15 | 129 |
| **B19** | ######## | 4/4/1984 | F | 101 | 1.7 | 34.94 | 96 | 88.3333 | 125 | 70 | 34 | 86 | 210 | 145 | 37 | 140 |
| **B1** | ######## | 2/11/1972 | F | 100 | 1.72 | 33.8 | 95 | 96.6667 | 130 | 80 | 38 | 84 | 170 | 105 | 50 | 120 |
| **B2** | ######## | 4/24/1985 | F | 135 | 1.75 | 44.08 | 102 | 90 | 120 | 75 | 36 | 87 | 173 | 110 | 42 | 98 |
| **B3** | 4/8/2014 | 9/30/1971 | F | 125 | 1.7 | 43.25 | 104 | 96.6667 | 120 | 85 | 40 | 91 | 173 | 108 | 54 | 87 |
| **B4** | ######## | 1/26/1978 | F | 130 | 1.7 | 44.98 | 101 | 90 | 130 | 70 | 35 | 108 | 172 | 98 | 54 | 100 |
| **B5** | ######## | 4/29/1974 | M | 136 | 1.83 | 40.61 | 109 | 103.333 | 140 | 85 | 31 | 75 | 185 | 113 | 62 | 46 |
| **MEAN** | | | | 126.33 | 1.709 | 43.165 | 106.667 | 95.463 | 128.0556 | 79.167 | 36.2778 | 88.1111 | 188.7222 | 114.7778 | 49.66667 | 110.3333333 |
| **STANDARD DEVIATION** | | | | 5.1892 | 0.015 | 1.5783 | 1.70543 | 1.76098 | 2.219156 | 1.819 | 0.78717 | 2.48116 | 6.797157 | 5.200274 | 2.887883 | 10.14889157 |
| **Obese subjects with METs (group 3: PO)** | | | | | | | | | | | | | | | | |
| **C13** | ######## | 5/16/1961 | M | 190 | 1.98 | 48.46 | 113 | 96.6667 | 130 | 80 | 39 | 141 | 192 | 80 | 26 | 434 |
| **C16** | ######## | 7/16/1967 | F | 140 | 1.57 | 56.79 | 108 | 105 | 135 | 90 | 45 | 87 | 248 | 172 | 48 | 127 |
| **C21** | 6/3/2014 | 4/11/1959 | M | 170 | 1.8 | 52.46 | 110 | 106.667 | 140 | 90 | 36 | 100 | 236 | 148 | 58 | 163 |
| **C 22** | ######## | 8/20/1960 | M | 131 | 1.7 | 45.32 | 107 | 83.3333 | 110 | 70 | 65 | 179 | 218 | 137 | 25 | 412 |
| **C 23** | ######## | 3/11/1970 | F | 126 | 1.7 | 43.59 | 103 | 98.3333 | 125 | 85 | 53 | 149 | 181 | 101 | 25 | 278 |
| **C 27** | ######## | 9/27/1943 | F | 135 | 1.5 | 60 | 114 | 110 | 150 | 90 | 81 | 226 | 167 | 80 | 47 | 201 |
| **C 28** | ######## | 3/9/1968 | F | 137 | 1.65 | 50.32 | 101 | 88.3333 | 115 | 75 | 45 | 116 | 185 | 108 | 35 | 210 |
| **C 30** | 9/1/2015 | 2/8/1952 | F | 84 | 1.57 | 34.07 | 97 | 101.667 | 125 | 90 | 38 | 87 | 206 | 104 | 42 | 300 |
| **C 32** | ######## | ######### | M | 135 | 1.73 | 45.1 | 103 | 105 | 145 | 85 | 43 | 130 | 234 | 114 | 30 | 504 |
| **C 33** | ######## | 1/28/1955 | F | 135 | 1.73 | 45.1 | 97 | 108.333 | 135 | 95 | 73 | 268 | 178 | 98 | 66 | 70 |
| **C 34** | ######## | 4/1/1944 | F | 110 | 1.63 | 41.4 | 98 | 85 | 115 | 70 | 51 | 111 | 211 | 140 | 33 | 190 |
| **C 36** | ######## | 7/26/1952 | M | 126 | 1.6 | 49.21 | 106 | 100 | 140 | 80 | 45 | 120 | 105 | 50 | 40 | 73 |
| **C 40** | ######## | 10/4/1992 | F | 116 | 1.66 | 42.09 | 100 | 96.6667 | 120 | 85 | 45 | 86 | 148 | 85 | 27 | 285 |
| **C1** | ######## | 4/6/1973 | M | 150 | 1.73 | 50.11 | 109 | 96.6667 | 130 | 80 | 39 | 86 | 268 | 202 | 35 | 155 |
| **C4** | 4/4/2014 | 1/18/1979 | M | 205 | 1.78 | 64.7 | 116 | 90 | 120 | 75 | 70 | 180 | 159 | 107 | 28 | 121 |
| **C5** | 4/8/2014 | ######### | M | 140 | 1.83 | 41.8 | 105 | 91.6667 | 115 | 80 | 80 | 172 | 161 | 95 | 32 | 199 |
| **C10** | ######## | 7/18/1974 | F | 130 | 1.57 | 52.74 | 104 | 98.3333 | 125 | 85 | 51 | 105 | 236 | 167 | 31 | 236 |
| **C11** | 6/3/2014 | 5/5/1970 | F | 145 | 1.68 | 51.37 | 101 | 106.667 | 140 | 90 | 49 | 107 | 197 | 107 | 51 | 197 |
| **MEAN** | | | | 139.17 | 1.689 | 48.591 | 105.111 | 98.2407 | 128.6111 | 83.056 | 52.6667 | 136.111 | 196.1111 | 116.3889 | 37.72222 | 230.8333333 |
| **STANDARD DEVIATION** | | | | 6.5196 | 0.027 | 1.7278 | 1.35735 | 1.89825 | 2.735794 | 1.7216 | 3.44423 | 12.1289 | 9.573892 | 8.937744 | 2.828202 | 28.45777172 |

# Table S2 Heat map of statistically significant biochemicals profiled in this study

Red and green shaded cells indicate p≤0.05 (red indicates that the mean values are significantly higher for that comparison; green values significantly lower).
Light red and light green shaded cells indicate 0.05<p<0.10 (light red indicates that the mean values trend higher for that comparison; light green values trend lower).

| | | | Fold of Change | | | |
|---|---|---|---|---|---|---|
| Super Pathway | Sub Pathway | Biochemical Name | Group Effect | OBESE_(O) VS HEALTHY_(H) | PATHOLOGICAL_OBESE_(PO) VS | PATHOLOGICAL_OBESE_(PO) VS OBESE_(O) |
| | Glutathione Metabolism | glutathione, reduced (GSH) | 1 | 0,9105 | 0,79 | 0,8677 |
| | | glutathione, oxidized (GSSG) | 1 | 0,8975 | 1,1182 | 1,2459 |
| | | cysteine-glutathione disulfide | 1 | 0,5533 | 0,778 | 1,406 |
| | | 5-oxoproline | 1 | 0,6461 | 0,904 | 1,3992 |
| | | 2-hydroxybutyrate/2-hydroxyisobutyrate | 1 | 0,6029 | 0,7829 | 1,2986 |
| | | ophthalmate | 1 | 0,7834 | 1,2228 | 1,5609 |
| Peptide | Gamma-glutamyl Amino Acid | gamma-glutamylcysteine | 1 | 0,2934 | 0,3488 | 1,1888 |
| | | gamma-glutamylglutamate | 1 | 0,8357 | 1,5015 | 1,7966 |
| | | gamma-glutamylglutamine | 1 | 0,6253 | 1,0681 | 1,7083 |
| | | gamma-glutamyl-alpha-lysine | 1 | 0,4842 | 0,5831 | 1,2044 |
| | | gamma-glutamyl-epsilon-lysine | 1 | 0,3083 | 0,5362 | 1,7393 |
| | | gamma-glutamylthreonine | 1 | 0,8249 | 1,3212 | 1,6017 |
| | | gamma-glutamylvaline | 1 | 0,662 | 1,1313 | 1,7089 |
| | Dipeptide | glycylvaline | 1 | 0,7219 | 0,705 | 0,9766 |
| | | isoleucylglycine | 1 | 0,7715 | 0,6525 | 0,8457 |
| | | leucylglycine | 1 | 0,4194 | 0,3218 | 0,7674 |
| | | phenylalanylglycine | 1 | 0,9061 | 0,9844 | 1,0863 |
| | | tryptophylglycine | 1 | 0,6617 | 0,4579 | 0,692 |
| | Acetylated Peptides | phenylacetylglutamine | 1 | 0,3888 | 0,3946 | 1,0147 |
| Carbohydrate | Glycolysis, Gluconeogenesis, and Pyruvate Metabolism | 1,5-anhydroglucitol (1,5-AG) | 1 | 0,657 | 0,5582 | 0,8497 |
| | | glucose | 1 | 0,5235 | 0,78 | 1,49 |
| | | Isobar: fructose 1,6-diphosphate, glucose 1,6-diphosphate, myo-inositol 1,4 or 1,3-diphosphate | 1 | 0,9551 | 0,9684 | 1,014 |
| | | dihydroxyacetone phosphate (DHAP) | 1 | 0,9522 | 1,2173 | 1,2785 |
| | | 3-phosphoglycerate | 1 | 0,7667 | 0,9008 | 1,1748 |
| | | phosphoenolpyruvate (PEP) | 1 | 0,6666 | 0,7848 | 1,1773 |
| | | pyruvate | 1 | 0,8248 | 0,8933 | 1,0831 |
| | | lactate | 1 | 0,7407 | 0,8387 | 1,1322 |
| | | glycerate | 1 | 0,623 | 0,6915 | 1,11 |
| | Pentose Phosphate Pathway | 6-phosphogluconate | 1 | 0,2181 | 0,2768 | 1,2692 |
| | | sedoheptulose-7-phosphate | 1 | 0,8542 | 0,8025 | 0,9394 |
| | Pentose Metabolism | ribose | 1 | 0,5837 | 0,799 | 1,3689 |
| | | ribitol | 1 | 0,3981 | 0,5041 | 1,2664 |
| | | ribonate | 1 | 0,7223 | 0,8447 | 1,1694 |
| | | arabitol/xylitol | 1 | 0,3728 | 0,5276 | 1,4152 |
| | | arabonate/xylonate | 1 | 0,6137 | 0,7316 | 1,1921 |
| | Glycogen Metabolism | maltotetraose | 1 | 0,4976 | 0,5048 | 1,0145 |
| | | maltotriose | 1 | 0,5393 | 0,5607 | 1,0397 |
| | | maltose | 1 | 0,5539 | 0,4863 | 0,878 |
| | Fructose, Mannose and Galactose Metabolism | fructose | 1 | 0,698 | 0,891 | 1,2765 |
| | | mannitol/sorbitol | 1 | 2,5502 | 13,1751 | 5,1662 |
| | | mannose | 1 | 0,6285 | 0,8687 | 1,3813 |
| | | galactonate | 1 | 0,5761 | 0,5506 | 0,9556 |
| | Nucleotide Sugar | UDP-glucose | 1 | 0,9439 | 1,0453 | 1,1074 |
| | | UDP-galactose | 1 | 0,9314 | 1,1332 | 1,2166 |
| | | UDP-glucuronate | 1 | 1,2257 | 1,103 | 0,8999 |
| | | UDP-N-acetylglucosamine | 1 | 1,0273 | 0,9954 | 0,9689 |
| | | UDP-N-acetylgalactosamine | 1 | 0,8643 | 0,8514 | 0,9851 |
| | Aminosugar Metabolism | glucuronate | 1 | 0,4583 | 0,6191 | 1,3511 |
| | | N-acetylglucosamine 6-phosphate | 1 | 0,4937 | 0,7716 | 1,563 |
| | | N-acetyl-glucosamine 1-phosphate | 1 | 0,5457 | 1,0782 | 1,9758 |
| | | N-acetylneuraminate | 1 | 0,703 | 0,9757 | 1,3878 |
| | | N-acetylglucosaminylasparagine | 1 | 0,7602 | 0,9187 | 1,2085 |
| | | erythronate* | 1 | 0,5297 | 0,7794 | 1,4714 |
| | | N-acetylglucosamine/N-acetylgalactosamine | 1 | 0,8125 | 0,9322 | 1,1473 |
| Energy | TCA Cycle | citrate | 1 | 0,5587 | 0,6543 | 1,1711 |
| | | alpha-ketoglutarate | 1 | 0,5185 | 0,8705 | 1,6789 |
| | | succinylcarnitine (C4-DC) | 1 | 0,8176 | 0,7535 | 0,9215 |
| | | succinate | 1 | 0,9591 | 0,9746 | 1,0162 |
| | | fumarate | 1 | 0,7467 | 0,8413 | 1,1268 |
| | | malate | 1 | 0,8955 | 0,9803 | 1,0948 |
| | | 2-methylcitrate/homocitrate | 1 | 0,7354 | 0,7518 | 1,0222 |
| | Oxidative Phosphorylation | acetylphosphate | 1 | 0,6986 | 0,8436 | 1,2076 |
| | | phosphate | 1 | 0,5865 | 0,6146 | 1,048 |
| | Medium Chain Fatty Acid | caproate (6:0) | 1 | 0,8955 | 0,726 | 0,8107 |
| | | heptanoate (7:0) | 1 | 0,8854 | 0,8253 | 0,9321 |
| | | caprylate (8:0) | 1 | 0,5399 | 0,5947 | 1,1014 |
| | | caprate (10:0) | 1 | 0,7386 | 0,7563 | 1,024 |
| | Long Chain Fatty Acid | myristate (14:0) | 1 | 0,796 | 0,7802 | 0,9801 |
| | | myristoleate (14:1n5) | 1 | 0,8219 | 0,8262 | 1,0052 |
| | | palmitate (16:0) | 1 | 0,8032 | 0,8577 | 1,0679 |
| | | palmitoleate (16:1n7) | 1 | 0,6144 | 0,6449 | 1,0497 |
| | | 10-heptadecenoate (17:1n7) | 1 | 0,7665 | 0,7959 | 1,0383 |
| | | 10-nonadecenoate (19:1n9) | 1 | 0,7595 | 0,7514 | 0,9893 |
| | | eicosenoate (20:1) | 1 | 0,6864 | 0,7034 | 1,0248 |
| | | erucate (22:1n9) | 1 | 0,5926 | 0,6996 | 1,1806 |
| | | oleate/vaccenate (18:1) | 1 | 0,6519 | 0,6826 | 1,0477 |
| | Polyunsaturated Fatty Acid (n3 and n6) | stearidonate (18:4n3) | 1 | 0,5167 | 0,4598 | 0,89 |
| | | eicosapentaenoate (EPA; 20:5n3) | 1 | 0,609 | 0,8587 | 1,41 |
| | | docosapentaenoate (n3 DPA; 22:5n3) | 1 | 0,6826 | 0,786 | 1,1515 |
| | | docosahexaenoate (DHA; 22:6n3) | 1 | 0,5692 | 0,7798 | 1,3696 |
| | | linoleate (18:2n6) | 1 | 0,6014 | 0,6468 | 1,0754 |
| | | linolenate [alpha or gamma; (18:3n3 or 6)] | 1 | 0,5601 | 0,6219 | 1,1105 |
| | | dihomo-linolenate (20:3n3 or n6) | 1 | 0,672 | 0,8891 | 1,323 |
| | | arachidonate (20:4n6) | 1 | 0,64 | 0,8258 | 1,2903 |
| | | docosapentaenoate (n6 DPA; 22:5n6) | 1 | 0,5854 | 0,6052 | 1,0338 |
| | | docosadienoate (22:2n6) | 1 | 0,6803 | 0,7181 | 1,0555 |
| | | dihomo-linoleate (20:2n6) | 1 | 0,7355 | 0,7587 | 1,0315 |
| | | mead acid (20:3n9) | 1 | 0,6096 | 0,5751 | 0,9434 |
| | Fatty Acid, Dicarboxylate | 2-hydroxyglutarate | 1 | 0,6735 | 0,998 | 1,4809 |
| | | maleate | 1 | 0,1281 | 0,1608 | 1,2557 |

| | | | | | | | |
|---|---|---|---|---|---|---|---|
| | | 3-carboxy-4-methyl-5-propyl-2-furanpropanoate (CMPF) | 1 | 0,4507 | 1,8672 | 4,1425 |
| | Fatty Acid Synthesis | malonylcarnitine | 1 | 0,8896 | 0,7714 | 0,8671 |
| | Fatty Acid Metabolism (also BCAA Metabolism) | butyrylcarnitine (C4) | 1 | 0,7332 | 0,8862 | 1,2086 |
| | | propionylcarnitine (C3) | 1 | 0,952 | 0,9743 | 1,0234 |
| | Fatty Acid Metabolism(Acyl Carnitine) | acetylcarnitine (C2) | 1 | 0,67 | 0,8852 | 1,3211 |
| | | 3-hydroxybutyrylcarnitine (1) | 1 | 0,7287 | 0,627 | 0,8605 |
| | | 3-hydroxybutyrylcarnitine (2) | 1 | 0,8406 | 1,0323 | 1,2281 |
| | | hexanoylcarnitine (C6) | 1 | 0,6538 | 0,8796 | 1,3453 |
| | | octanoylcarnitine (C8) | 1 | 0,819 | 0,859 | 1,0489 |
| | | decanoylcarnitine (C10) | 1 | 0,7719 | 0,8161 | 1,0572 |
| | | cis-4-decenoylcarnitine (C10:1) | 1 | 0,5254 | 0,7001 | 1,3324 |
| | | laurylcarnitine (C12) | 1 | 0,7334 | 0,8947 | 1,2199 |
| | | myristoylcarnitine (C14) | 1 | 0,7102 | 0,8584 | 1,2086 |
| | | palmitoylcarnitine (C16) | 1 | 0,6801 | 0,8435 | 1,2403 |
| | | palmitoleoylcarnitine (C16:1)* | 1 | 0,6329 | 0,7477 | 1,1815 |
| | | linoleoylcarnitine (C18:2)* | 1 | 0,4907 | 0,5937 | 1,2099 |
| | | oleoylcarnitine (C18:1) | 1 | 0,5756 | 0,6793 | 1,1803 |
| | | myristoleoylcarnitine (C14:1)* | 1 | 0,7902 | 0,8283 | 1,0482 |
| | | arachidoylcarnitine (C20)* | 1 | 0,8982 | 1,0309 | 1,1477 |
| | | arachidonoylcarnitine (C20:4) | 1 | 0,791 | 1,1218 | 1,4181 |
| | Carnitine Metabolism | deoxycarnitine | 1 | 0,6329 | 0,6927 | 1,0946 |
| | | carnitine | 1 | 0,753 | 0,8196 | 1,0884 |
| | Ketone Bodies | 3-hydroxybutyrate (BHBA) | 1 | 0,3902 | 0,3279 | 0,8403 |
| | Fatty Acid, Monohydroxy | 13-HODE + 9-HODE | 1 | 0,7041 | 0,7872 | 1,1179 |
| | Eicosanoid | 6-keto prostaglandin F1alpha | 1 | 1,1436 | 1,7401 | 1,5215 |
| | | 15-HETE | 1 | 0,7309 | 1,2633 | 1,7282 |
| | Endocannabinoid | oleoyl ethanolamide | 1 | 0,7324 | 0,7472 | 1,0202 |
| | Inositol Metabolism | myo-inositol | 1 | 0,771 | 0,7971 | 1,0348 |
| | Phospholipid Metabolism | choline | 1 | 0,8446 | 1,025 | 1,2135 |
| | | choline phosphate | 1 | 0,7411 | 0,927 | 1,2508 |
| | | cytidine 5'-diphosphocholine | 1 | 0,7675 | 0,7213 | 0,9398 |
| | | glycerophosphorylcholine (GPC) | 1 | 1,1283 | 1,3767 | 1,2202 |
| | | phosphoethanolamine | 1 | 0,6956 | 0,8006 | 1,151 |
| | | cytidine-5'-diphosphoethanolamine | 1 | 0,7169 | 0,7054 | 0,984 |
| | | glycerophosphoethanolamine | 1 | 0,7826 | 1,0496 | 1,3412 |
| | | trimethylamine N-oxide | 1 | 0,4647 | 0,5189 | 1,1166 |
| | | glycerophosphoinositol* | 1 | 0,6834 | 0,6087 | 0,89 |
| | | 1,2-dipalmitoyl-GPC (16:0/16:0) | 1 | 0,6984 | 0,921 | 1,3188 |
| | | 1,2-dipalmitoyl-GPE (16:0/16:0)* | 1 | 0,5557 | 0,7746 | 1,3938 |
| | | 1-palmitoyl-2-oleoyl-GPC (16:0/18:1) | 1 | 0,8633 | 1,0016 | 1,1602 |
| | | 1-palmitoyl-2-linoleoyl-GPC (16:0/18:2) | 1 | 0,8498 | 0,9106 | 1,0715 |
| | | 1-stearoyl-2-arachidonoyl-GPC (18:0/20:4) | 1 | 0,6342 | 0,9524 | 1,5016 |
| | | 1-stearoyl-2-oleoyl-GPC (18:0/18:1) | 1 | 0,7554 | 0,9112 | 1,2064 |
| | | 1,2-dioleoyl-GPC (18:1/18:1) | 1 | 0,7798 | 0,8107 | 1,0396 |
| | | 1-palmitoyl-2-arachidonoyl-GPC (16:0/20:4n6) | 1 | 0,693 | 0,8964 | 1,2936 |
| | | 1-stearoyl-2-linoleoyl-GPC (18:0/18:2)* | 1 | 0,7834 | 0,9391 | 1,1987 |
| | | 1-palmitoyl-2-palmitoleoyl-GPC (16:0/16:1)* | 1 | 1,0731 | 1,223 | 1,1397 |
| | | 1-stearoyl-2-arachidonoyl-GPI (18:0/20:4) | 1 | 0,8264 | 1,2414 | 1,5022 |
| | | 1-oleoyl-2-linoleoyl-GPC (18:1/18:2)* | 1 | 0,7484 | 0,7876 | 1,0524 |
| | | 1-palmitoyl-2-arachidonoyl-GPI (16:0/20:4)* | 1 | 0,9459 | 0,9118 | 0,964 |
| | | 1-palmitoyl-2-oleoyl-GPE (16:0/18:1) | 1 | 0,8476 | 0,906 | 1,0688 |
| | | 1-stearoyl-2-arachidonoyl-GPE (18:0/20:4) | 1 | 0,8252 | 1,0353 | 1,2546 |
| | | 1-stearoyl-2-oleoyl-GPE (18:0/18:1) | 1 | 0,856 | 1,0496 | 1,2262 |
| | | 1-palmitoyl-2-arachidonoyl-GPE (16:0/20:4)* | 1 | 0,865 | 0,9296 | 1,0746 |
| | | 1-palmitoyl-2-linoleoyl-GPE (16:0/18:2) | 1 | 0,8183 | 0,753 | 0,9202 |
| | | 1-stearoyl-2-linoleoyl-GPE (18:0/18:2)* | 1 | 0,8621 | 0,9628 | 1,1167 |
| | | 1-palmitoyl-2-stearoyl-GPC (16:0/18:0) | 1 | 0,5824 | 0,834 | 1,4319 |
| | | 1,2-dioleoyl-GPE (18:1/18:1) | 1 | 0,8626 | 0,9025 | 1,0462 |
| | | 1-stearoyl-2-oleoyl-GPG (18:0/18:1) | 1 | 0,7209 | 1,0062 | 1,3957 |
| | | 1,2-dilinoleoyl-GPC (18:2/18:2) | 1 | 0,6887 | 0,6175 | 0,8967 |
| | | 1-oleoyl-2-linoleoyl-GPE (18:1/18:2)* | 1 | 0,7854 | 0,6868 | 0,8745 |
| | | 1-linoleoyl-2-arachidonoyl-GPC (18:2/20:4n6)* | 1 | 0,5833 | 0,6506 | 1,1155 |
| | | 1-stearoyl-2-linoleoyl-GPS (18:0/18:2) | 1 | 0,8614 | 1,0575 | 1,2277 |
| | | 1-oleoyl-2-arachidonoyl-GPE (18:1/20:4)* | 1 | 0,804 | 0,8962 | 1,1147 |
| | | 1-oleoyl-2-arachidonoyl-GPI (18:1/20:4) * | 1 | 0,9686 | 0,9344 | 0,9647 |
| | Phosphatidylserine (PS) | 1-stearoyl-2-arachidonoyl-GPS (18:0/20:4) | 1 | 0,7531 | 1,0041 | 1,3333 |
| | | 1-stearoyl-2-oleoyl-GPS (18:0/18:1) | 1 | 0,722 | 0,9226 | 1,2778 |
| Lipid | Lysolipid | 1-palmitoyl-GPC (16:0) | 1 | 0,5849 | 0,7111 | 1,2158 |
| | | 2-palmitoyl-GPC (16:0)* | 1 | 0,6686 | 0,8627 | 1,2903 |
| | | 1-palmitoleoyl-GPC (16:1)* | 1 | 0,4165 | 0,448 | 1,0709 |
| | | 2-palmitoleoyl-GPC (16:1)* | 1 | 1,032 | 1,1464 | 1,1108 |
| | | 1-stearoyl-GPC (18:0) | 1 | 0,5739 | 0,7337 | 1,2784 |
| | | 1-oleoyl-GPC (18:1) | 1 | 0,5338 | 0,6243 | 1,1695 |
| | | 1-linoleoyl-GPC (18:2) | 1 | 0,6458 | 0,5818 | 0,901 |
| | | 1-arachidonoyl-GPC (20:4n6)* | 1 | 0,7038 | 0,7937 | 1,1277 |
| | | 1-palmitoyl-GPE (16:0) | 1 | 0,5343 | 1,009 | 1,8884 |
| | | 1-stearoyl-GPE (18:0) | 1 | 0,6868 | 1,3916 | 2,0263 |
| | | 1-oleoyl-GPE (18:1) | 1 | 0,6491 | 0,9201 | 1,4176 |
| | | 1-linoleoyl-GPE (18:2)* | 1 | 0,9047 | 0,604 | 0,6676 |
| | | 1-arachidonoyl-GPE (20:4n6)* | 1 | 0,9047 | 1,0085 | 1,1148 |
| | | 1-stearoyl-GPI (18:0) | 1 | 0,6628 | 1,1757 | 1,7738 |
| | | 1-stearoyl-GPS (18:0)* | 1 | 0,5028 | 1,0762 | 2,1403 |
| | Plasmalogen | 1-(1-enyl-palmitoyl)-2-oleoyl-GPE (P-16:0/18:1)* | 1 | 0,9598 | 1,0265 | 1,0695 |
| | | 1-(1-enyl-palmitoyl)-2-linoleoyl-GPE (P-16:0/18:2)* | 1 | 0,9408 | 0,8587 | 0,9127 |
| | | 1-(1-enyl-palmitoyl)-2-palmitoyl-GPC (P-16:0/16:0)* | 1 | 0,7662 | 1,3105 | 1,7103 |
| | | 1-(1-enyl-palmitoyl)-2-palmitoleoyl-GPC (P-16:0/16:1)* | 1 | 0,9391 | 1,269 | 1,3513 |
| | | 1-(1-enyl-palmitoyl)-2-arachidonoyl-GPE (P-16:0/20:4)* | 1 | 0,9845 | 1,3144 | 1,3352 |
| | | 1-(1-enyl-palmitoyl)-2-oleoyl-GPC (P-16:0/18:1)* | 1 | 0,794 | 1,0023 | 1,2624 |
| | | 1-(1-enyl-stearoyl)-2-oleoyl-GPE (P-18:0/18:1) | 1 | 0,7632 | 0,7778 | 1,019 |
| | | 1-(1-enyl-stearoyl)-2-linoleoyl-GPE (P-18:0/18:2)* | 1 | 0,7595 | 0,6394 | 0,8419 |
| | | 1-(1-enyl-palmitoyl)-2-arachidonoyl-GPC (P-16:0/20:4)* | 1 | 0,8315 | 1,3102 | 1,5756 |
| | | 1-(1-enyl-palmitoyl)-2-linoleoyl-GPC (P-16:0/18:2)* | 1 | 0,8564 | 1,1088 | 1,2947 |
| | | 1-(1-enyl-stearoyl)-2-arachidonoyl-GPE (P-18:0/20:4)* | 1 | 0,8307 | 1,12 | 1,3483 |
| | Lysoplasmalogen | 1-(1-enyl-palmitoyl)-GPE (P-16:0)* | 1 | 0,8126 | 1,6608 | 2,0438 |
| | | 1-(1-enyl-oleoyl)-GPE (P-18:1)* | 1 | 0,7024 | 1,6888 | 2,4044 |
| | | 1-(1-enyl-stearoyl)-GPE (P-18:0)* | 1 | 0,6736 | 1,2756 | 1,8931 |
| | | 1-(1-enyl-oleoyl)-2-oleoyl-GPE (P-18:1/18:1)* | 1 | 0,8247 | 0,9042 | 1,0964 |
| | | 1-(1-enyl-oleoyl)-2-linoleoyl-GPE (P-18:1/18:2)* | 1 | 0,8442 | 0,7229 | 0,8563 |

| | | | | | | |
|---|---|---|---|---|---|---|
| | Glycerolipid Metabolism | glycerol | 1 | 0,7238 | 0,825 | 1,1398 |
| | | glycerol 3-phosphate | 1 | 0,8259 | 0,9142 | 1,1069 |
| | | glycerophosphoglycerol | 1 | 0,8827 | 1,1881 | 1,346 |
| | Monoacylglycerol | 1-oleoylglycerol (18:1) | 1 | 0,8041 | 1,1463 | 1,4256 |
| | Diacylglycerol | diacylglycerol (12:0/18:1, 14:0/16:1, 16:0/14:1) [2]* | 1 | 0,7989 | 0,8463 | 1,0592 |
| | | diacylglycerol (14:0/18:1, 16:0/16:1) [2]* | 1 | 0,8892 | 1,0695 | 1,2028 |
| | | diacylglycerol (16:1/18:2 [2], 16:0/18:3 [1])* | 1 | 0,9983 | 1,084 | 1,0858 |
| | | oleoyl-arachidonoyl-glycerol (18:1/20:4) [2]* | 1 | 0,8966 | 1,3348 | 1,4888 |
| | | palmitoyl-arachidonoyl-glycerol (16:0/20:4) [2]* | 1 | 0,8464 | 1,0298 | 1,2167 |
| | | palmitoleoyl-linoleoyl-glycerol (16:1/18:2) [1]* | 1 | 0,738 | 0,7728 | 1,0471 |
| | | palmitoyl-oleoyl-glycerol (16:0/18:1) [2]* | 1 | 0,8142 | 1,0333 | 1,269 |
| | | palmitoleoyl-oleoyl-glycerol (16:1/18:1) [2]* | 1 | 0,9194 | 1,0842 | 1,1792 |
| | | palmitoyl-linoleoyl-glycerol (16:0/18:2) [2]* | 1 | 0,8716 | 1,0332 | 1,1854 |
| | | stearoyl-arachidonoyl-glycerol (18:0/20:4) [2]* | 1 | 0,8658 | 1,1684 | 1,3495 |
| | | oleoyl-oleoyl-glycerol (18:1/18:1) [1]* | 1 | 0,764 | 0,6966 | 0,9118 |
| | | oleoyl-oleoyl-glycerol (18:1/18:1) [2]* | 1 | 0,8398 | 1,0248 | 1,2203 |
| | Sphingolipid Metabolism | N-palmitoyl-sphinganine (d18:0/16:0) | 1 | 0,7069 | 0,9926 | 1,4042 |
| | | N-palmitoyl-sphingadienine (d18:2/16:0)* | 1 | 0,9895 | 1,3386 | 1,3527 |
| | | N-behenoyl-sphingadienine (d18:2/22:0)* | 1 | 1,0772 | 1,3828 | 1,2837 |
| | | myristoyl dihydrosphingomyelin (d18:0/14:0)* | 1 | 0,9212 | 0,8784 | 0,9536 |
| | | palmitoyl dihydrosphingomyelin (d18:0/16:0)* | 1 | 0,7283 | 0,9108 | 1,2506 |
| | | behenoyl dihydrosphingomyelin (d18:0/22:0)* | 1 | 0,6262 | 0,8615 | 1,3755 |
| | | palmitoyl sphingomyelin (d18:1/16:0) | 1 | 0,7851 | 0,9449 | 1,2036 |
| | | stearoyl sphingomyelin (d18:1/18:0) | 1 | 0,8528 | 1,0054 | 1,1789 |
| | | behenoyl sphingomyelin (d18:1/22:0)* | 1 | 0,8327 | 1,0682 | 1,2831 |
| | | tricosanoyl sphingomyelin (d18:1/23:0)* | 1 | 0,8152 | 0,9784 | 1,2001 |
| | | lignoceroyl sphingomyelin (d18:1/24:0) | 1 | 0,6954 | 0,865 | 1,2439 |
| | | sphingomyelin (d18:1/14:0, d16:1/16:0)* | 1 | 0,8752 | 1,0165 | 1,1615 |
| | | sphingomyelin (d18:2/14:0, d18:1/14:1)* | 1 | 1,0876 | 1,1442 | 1,052 |
| | | sphingomyelin (d17:1/16:0, d18:1/15:0, d16:1/17:0)* | 1 | 0,8546 | 0,9953 | 1,1647 |
| | | sphingomyelin (d18:2/16:0, d18:1/16:1)* | 1 | 0,983 | 1,162 | 1,182 |
| | | sphingomyelin (d18:1/17:0, d17:1/18:0, d19:1/16:0) | 1 | 0,7755 | 0,8811 | 1,1362 |
| | | sphingomyelin (d18:1/18:1, d18:2/18:0) | 1 | 0,9868 | 1,04 | 1,0539 |
| | | sphingomyelin (d18:1/20:0, d16:1/22:0)* | 1 | 0,7954 | 1,0903 | 1,3708 |
| | | sphingomyelin (d18:1/20:1, d18:2/20:0)* | 1 | 1,0491 | 1,1915 | 1,1357 |
| | | sphingomyelin (d18:1/21:0, d17:1/22:0, d16:1/23:0)* | 1 | 0,8694 | 1,0967 | 1,2615 |
| | | sphingomyelin (d18:1/22:1, d18:2/22:0, d16:1/24:1)* | 1 | 0,9519 | 1,2045 | 1,2654 |
| | | sphingomyelin (d18:2/23:0, d18:1/23:1, d17:1/24:1)* | 1 | 0,9276 | 1,1125 | 1,1993 |
| | | sphingomyelin (d18:1/24:1, d18:2/24:0)* | 1 | 0,69 | 0,8398 | 1,2171 |
| | | sphingomyelin (d18:2/24:1, d18:1/24:2)* | 1 | 0,8377 | 0,9144 | 1,0915 |
| | | sphingosine | 1 | 0,8152 | 1,1275 | 1,3831 |
| | | N-palmitoyl-sphingosine (d18:1/16:0) | 1 | 0,7992 | 1,1548 | 1,445 |
| | | N-stearoyl-sphingadienine (d18:2/18:0)* | 1 | 1,2615 | 1,6002 | 1,2685 |
| | | glycosyl-N-palmitoyl-sphingosine (d18:1/16:0) | 1 | 0,7304 | 1,028 | 1,4075 |
| | | lactosyl-N-palmitoyl-sphingosine (d18:1/16:0) | 1 | 0,6909 | 0,6879 | 0,9957 |
| | | sphingomyelin (d18:2/23:1)* | 1 | 0,896 | 0,8757 | 0,9773 |
| | | sphingomyelin (d18:2/21:0, d16:2/23:0)* | 1 | 1,0285 | 1,1994 | 1,1662 |
| | | sphingomyelin (d18:2/24:2)* | 1 | 0,9998 | 0,8957 | 0,8959 |
| | | N-nervonoyl-hexadecasphingosine (d16:1/24:1)* | 1 | 0,7779 | 1,0241 | 1,3164 |
| | | N-nervonoyl-sphingadiene (d18:2/24:1)* | 1 | 0,9953 | 1,1869 | 1,1924 |
| | | sphingomyelin (d18:1/22:2, d18:2/22:1, d16:1/24:2)* | 1 | 0,9162 | 0,8448 | 0,9221 |
| | | sphingomyelin (d18:0/18:0, d19:0/17:0)* | 1 | 0,7586 | 0,9366 | 1,2347 |
| | | sphingomyelin (d18:1/19:0, d19:1/18:0)* | 1 | 0,8791 | 1,13 | 1,2854 |
| | | hexadecasphingosine (d16:1)* | 1 | 0,9356 | 1,4164 | 1,514 |
| | | N-palmitoyl-heptadecasphingosine (d17:1/16:0)* | 1 | 0,8483 | 1,1948 | 1,4084 |
| | | sphingadienine* | 1 | 0,9794 | 1,5098 | 1,5416 |
| | Mevalonate Metabolism | 3-hydroxy-3-methylglutarate | 1 | 0,5249 | 0,4608 | 0,8778 |
| | Sterol | cholesterol | 1 | 0,7747 | 0,955 | 1,2328 |
| | | 4-cholesten-3-one | 1 | 0,8881 | 0,9588 | 1,0796 |
| | Steroid | pregnen-diol disulfate* | 1 | 0,3036 | 0,4019 | 1,3238 |
| | | cortisol | 1 | 5,4215 | 3,0474 | 0,5621 |
| | | dehydroisoandrosterone sulfate (DHEA-S) | 1 | 0,4404 | 0,6533 | 1,4834 |
| | | androsterone sulfate | 1 | 0,4029 | 0,5689 | 1,4119 |
| | | androstenediol (3beta,17beta) disulfate (1) | 1 | 0,4061 | 0,5923 | 1,458 |
| | Primary Bile Acid Metabolism | cholate | 1 | 0,0751 | 0,0751 | 1 |
| | | glycocholate | 1 | 0,028 | 0,028 | 1 |
| | | taurocholate | 1 | 1 | 1 | 1 |
| | | glycochenodeoxycholate | 1 | 0,0097 | 0,0165 | 1,707 |
| | | taurochenodeoxycholate | 1 | 0,0499 | 0,0499 | 1 |
| | Secondary Bile Acid Metabolism | glycodeoxycholate | 1 | 0,0021 | 0,0029 | 1,3726 |
| | | taurodeoxycholate | 1 | 1 | 1 | 1 |
| | | glycolithocholate | 1 | 1 | 1 | 1 |
| | | glycolithocholate sulfate* | 1 | 0,1473 | 0,1473 | 0,9999 |
| | | glycoursodeoxycholate | 1 | 0,1163 | 0,1808 | 1,5544 |
| | Ceramides | ceramide (d14:1/22:0, d16:1/20:0)* | 1 | 0,876 | 1,269 | 1,4487 |
| | | ceramide (d18:1/14:0, d16:1/16:0)* | 1 | 0,9009 | 1,2274 | 1,3624 |
| | | ceramide (d18:1/17:0, d17:1/18:0)* | 1 | 0,7945 | 1,1014 | 1,3862 |
| | | ceramide (d18:1/20:0, d16:1/22:0, d20:1/18:0)* | 1 | 0,8692 | 1,216 | 1,399 |
| Nucleotide | Purine Metabolism, (Hypo)Xanthine/Inosine containing | inosine | 1 | 0,9163 | 0,9924 | 1,083 |
| | | hypoxanthine | 1 | 0,7871 | 0,8365 | 1,0627 |
| | | xanthine | 1 | 0,7781 | 0,9824 | 1,2625 |
| | | xanthosine | 1 | 0,3148 | 0,6435 | 2,0438 |
| | | urate | 1 | 0,7231 | 0,8799 | 1,2168 |
| | | allantoin | 1 | 0,3542 | 0,4502 | 1,2708 |
| | Purine Metabolism, Adenine containing | adenosine 5'-monophosphate (AMP) | 1 | 0,7263 | 0,2816 | 0,3877 |
| | | adenosine 3'-monophosphate (3'-AMP) | 1 | 0,6294 | 0,674 | 1,0708 |
| | | adenosine | 1 | 0,3677 | 0,2581 | 0,702 |
| | | adenine | 1 | 0,6567 | 0,8056 | 1,2268 |
| | Purine Metabolism, Guanine containing | guanosine 5'- monophosphate (5'-GMP) | 1 | 0,6106 | 0,6631 | 1,0859 |
| | | guanosine | 1 | 0,8988 | 1,0116 | 1,1255 |
| | | guanine | 1 | 0,6932 | 0,8172 | 1,1787 |
| | | 7-methylguanine | 1 | 0,6115 | 0,6758 | 1,1052 |
| | | N2,N2-dimethylguanosine | 1 | 0,4762 | 0,6242 | 1,3109 |
| | Pyrimidine Metabolism, Orotate containing | orotate | 1 | 0,5469 | 0,6352 | 1,1615 |
| | | orotidine | 1 | 0,439 | 3,109 | 7,0813 |
| | | uridine 5'-monophosphate (UMP) | 1 | 0,857 | 0,598 | 0,6978 |
| | | uridine | 1 | 0,845 | 0,9972 | 1,1801 |
| | | uracil | 1 | 0,7734 | 1,276 | 1,6498 |

| | | | | | | |
|---|---|---|---|---|---|---|
| | Pyrimidine Metabolism, Uracil containing | pseudouridine | 1 | 0,6776 | 0,8787 | 1,2968 |
| | | 5-methyluridine (ribothymidine) | 1 | 0,3801 | 0,4124 | 1,0848 |
| | | 3-ureidopropionate | 1 | 0,5373 | 0,7741 | 1,4408 |
| | | beta-alanine | 1 | 0,8075 | 0,931 | 1,1529 |
| | Pyrimidine Metabolism, Cytidine containing | cytidine 5'-monophosphate (5'-CMP) | 1 | 0,8403 | 0,9134 | 1,087 |
| | | cytidine 3'-monophosphate (3'-CMP) | 1 | 0,4349 | 0,6864 | 1,5783 |
| | | cytidine | 1 | 0,918 | 0,8662 | 0,9436 |
| | | cytosine | 1 | 0,4221 | 0,8322 | 1,9718 |
| | | 3-methylcytidine | 1 | 0,4754 | 0,5557 | 1,1691 |
| | | 2'-deoxycytidine | 1 | 0,455 | 0,5083 | 1,1171 |
| | Pyrimidine Metabolism, Thymine containing | thymidine | 1 | 0,9163 | 1,1002 | 1,2006 |
| | | 3-aminoisobutyrate | 1 | 0,7085 | 0,5688 | 0,8028 |
| | Purine and Pyrimidine Metabolism | methylphosphate | 1 | 0,864 | 0,9754 | 1,1289 |
| Cofactors and Vitamins | Nicotinate and Nicotinamide Metabolism | quinolinate | 1 | 0,3957 | 1,1902 | 3,0109 |
| | | nicotinamide | 1 | 0,834 | 0,9299 | 1,115 |
| | | nicotinamide ribonucleotide (NMN) | 1 | 0,6874 | 0,4112 | 0,5983 |
| | | nicotinamide riboside | 1 | 0,7608 | 0,3702 | 0,4865 |
| | | nicotinamide adenine dinucleotide (NAD+) | 1 | 0,8438 | 0,3855 | 0,4568 |
| | | 1-methylnicotinamide | 1 | 1,0265 | 1,1297 | 1,1005 |
| | | trigonelline (N'-methylnicotinate) | 1 | 0,5294 | 0,7344 | 1,3872 |
| | | N1-Methyl-2-pyridone-5-carboxamide | 1 | 0,7347 | 1,0697 | 1,4559 |
| | | N1-Methyl-4-pyridone-3-carboxamide | 1 | 0,6935 | 1,1169 | 1,6106 |
| | Pantothenate and CoA Metabolism | pantothenate | 1 | 0,8189 | 1,1903 | 1,4536 |
| | Ascorbate and Aldarate Metabolism | threonate | 1 | 0,3678 | 0,2435 | 0,6621 |
| | | gulonate* | 1 | 0,4949 | 0,4502 | 0,9097 |
| | Tocopherol Metabolism | alpha-tocopherol | 1 | 0,6014 | 0,9804 | 1,6302 |
| | | gamma-tocopherol/beta-tocopherol | 1 | 0,5782 | 0,8451 | 1,4616 |
| | Hemoglobin and Porphyrin Metabolism | heme | 1 | 0,4072 | 0,4737 | 1,1634 |
| | | biliverdin | 1 | 0,445 | 0,5221 | 1,1734 |
| | Vitamin A Metabolism | retinol (Vitamin A) | 1 | 0,8302 | 1,3268 | 1,5981 |
| Xenobiotics | Benzoate Metabolism | hippurate | 1 | 0,4435 | 0,4706 | 1,0611 |
| | | 3-hydroxyhippurate | 1 | 1,5201 | 1,4781 | 0,9724 |
| | | benzoate | 1 | 0,8382 | 0,7877 | 0,9398 |
| | | catechol sulfate | 1 | 0,4662 | 0,4947 | 1,061 |
| | | 4-methylcatechol sulfate | 1 | 0,6063 | 0,2414 | 0,3981 |
| | | methyl-4-hydroxybenzoate sulfate | 1 | 0,1767 | 0,4732 | 2,6858 |
| | | p-cresol sulfate | 1 | 0,3569 | 0,227 | 0,6221 |
| | Xanthine Metabolism | caffeine | 1 | 1,2317 | 1,4584 | 1,184 |
| | | paraxanthine | 1 | 0,9998 | 0,9998 | 1 |
| | | theobromine | 1 | 0,7602 | 0,7694 | 1,0121 |
| | | theophylline | 1 | 0,8727 | 1,1006 | 1,2612 |
| | | 1-methylurate | 1 | 0,3318 | 0,6561 | 1,9772 |
| | | 7-methylurate | 1 | 0,5332 | 0,7626 | 1,4303 |
| | | 1-methylxanthine | 1 | 0,7969 | 0,9744 | 1,2227 |
| | | 3-methylxanthine | 1 | 0,8391 | 0,8798 | 1,0484 |
| | | 5-acetylamino-6-amino-3-methyluracil | 1 | 0,488 | 0,819 | 1,6783 |
| | | 5-acetylamino-6-formylamino-3-methyluracil | 1 | 0,6319 | 0,686 | 1,0856 |
| | Tobacco Metabolite | cotinine | 1 | 0,8689 | 0,5746 | 0,6613 |
| | | hydroxycotinine | 1 | 1,0477 | 0,7702 | 0,7351 |
| | Food Component/Plant | gluconate | 1 | 0,2112 | 0,4664 | 2,208 |
| | | beta-guanidinopropanoate | 1 | 0,6488 | 0,7763 | 1,1964 |
| | | ergothioneine | 1 | 0,5046 | 0,6299 | 1,2483 |
| | | piperine | 1 | 0,5558 | 0,8929 | 1,6065 |
| | | quinate | 1 | 0,6652 | 0,8277 | 1,2443 |
| | | acesulfame | 1 | 0,9255 | 0,9341 | 1,0092 |
| | | stachydrine | 1 | 0,2613 | 0,2515 | 0,9639 |
| | | tartarate | 1 | 0,4937 | 0,5083 | 1,0296 |
| | | methyl glucopyranoside (alpha + beta) | 1 | 0,8624 | 0,5556 | 0,6443 |
| | Bacterial/Fungal | tartronate (hydroxymalonate) | 1 | 0,7755 | 0,895 | 1,1541 |
| | Drug | azithromycin | 1 | 4,2106 | 4,5808 | 1,0879 |
| | | 2-hydroxyacetaminophen sulfate* | 1 | 1 | 1 | 1 |
| | | 2-methoxyacetaminophen sulfate* | 1 | 1 | 1 | 1 |
| | | 3-(cystein-S-yl)acetaminophen* | 1 | 1 | 1 | 1 |
| | | 4-acetaminophen sulfate | 1 | 1,6822 | 13,6614 | 8,1212 |
| | | 4-acetamidophenol | 1 | 1,3081 | 3,5372 | 2,7041 |
| | | 4-acetamidophenylglucuronide | 1 | 1 | 1,2898 | 1,2898 |
| | | escitalopram | 1 | 1 | 1,6444 | 1,6444 |
| | | fluoxetine | 1 | 116,5359 | 6,321 | 0,0542 |
| | | gabapentin | 1 | 1 | 1 | 1 |
| | | lamotrigine | 1 | 1 | 1 | 1 |
| | | hydroxybupropion | 1 | 1 | 1 | 1 |
| | | hydroxypioglitazone (M-IV) | 1 | 1 | 1 | 1 |
| | | lidocaine | 1 | 0,515 | 0,57 | 1,1069 |
| | | metformin | 1 | 1 | 1,5735 | 1,5735 |
| | | N-ethylglycinexylidide | 1 | 0,416 | 0,765 | 1,8389 |
| | | norfluoxetine | 1 | 8,4469 | 2,583 | 0,3058 |
| | | oxypurinol | 1 | 0,7864 | 281,5818 | 358,0538 |
| | | pioglitazone | 1 | 1 | 1 | 1 |
| | | pseudoephedrine | 1 | 0,6312 | 0,9505 | 1,5058 |
| | | quetiapine | 1 | 1,1353 | 1 | 0,8808 |
| | | rocuronium | 1 | 0,6723 | 0,5699 | 0,8478 |
| | Chemical | O-sulfo-L-tyrosine | 1 | 0,5031 | 0,6758 | 1,3432 |
| | | HEPES | 1 | 1 | 3,0592 | 3,0592 |
| | | trizma acetate | 1 | 0,4299 | 0,7419 | 1,7258 |
| | | N-methylpipecolate | 1 | 0,5582 | 0,923 | 1,6534 |
| | | thioproline | 1 | 0,3995 | 0,4576 | 1,1455 |